

THE EXTRAORDINARY PHASES OF LIQUID ^3He

Nobel Lecture, December 7, 1996

by

DAVID M. LEE

Laboratory of Atomic and Solid State Physics, Dept. of Physics,
Cornell University, Ithaca, N.Y. 14853, USA

INTRODUCTION

Modern low temperature physics began with the liquefaction of helium¹ by Kamerlingh Onnes and the discovery of superconductivity² at the University of Leiden in the early part of the 20th century. There were really two surprises that came out of this early work. One was that essentially all of the electrical resistance of metals like mercury, lead, and tin abruptly vanished at definite transition temperatures. This was the first evidence for superconductivity. The other surprise was that, in contrast to other known liquids, liquid helium never solidified under its own vapor pressure. Helium is an inert gas so that the interactions between the helium atoms are very weak; thus the liquid phase itself is very weakly bound and the normal boiling point (4.2 K) is very low. The small atomic masses and the weak interaction lead to large amplitude quantum mechanical zero point vibrations which do not permit the liquid to freeze into the crystalline state. Only if a pressure of at least 25 atmospheres is applied will liquid ^4He solidify.³ It is thus possible, in principle, to study liquid ^4He all the way down to the neighborhood of absolute zero.

Quantum mechanics is of great importance in determining the macroscopic properties of liquid ^4He . Indeed, liquid helium belongs to a class of fluids known as quantum fluids, as distinct from classical fluids. In a quantum fluid the thermal de Broglie wavelength $\lambda_T = h(2\pi mkT)^{-\frac{1}{2}}$ is comparable to or greater than the mean interparticle distance. There is then a strong overlap between the wave functions of adjacent atoms, so quantum statistics will have important consequences. ^4He atoms contain even numbers of elementary particles and thus obey Bose-Einstein statistics, which means that any number of atoms can aggregate in a single quantum state in the non-interacting particle approximation. In fact macroscopic numbers of atoms in a quantum fluid can fall into the lowest energy state even at finite temperatures. This phenomenon is called Bose-Einstein condensation. On the other hand ^3He atoms, each of which contains an odd number of elementary particles, must obey Fermi-Dirac statistics: only one atom can occupy a given quantum state. Therefore one should expect a very large difference between the behavior of liquid ^4He and that of liquid ^3He for low temperatures where the thermal de Broglie wavelength becomes greater than the mean interparticle distance.

A remarkable phase transition was discovered in liquid ^4He under saturat-

ed vapor pressure at 2.17 K. As the liquid cooled through this temperature, all boiling ceased and the liquid became perfectly quiescent.⁴ We now know that this effect occurs because the liquid helium becomes an enormously good heat conductor so that thermal inhomogeneities which can give rise to bubble nucleation are absent. The specific heat vs. temperature curve of liquid ^4He was shaped like the Greek letter lambda, characteristic of a second order phase transition at 2.17 K. This temperature is called the lambda point.^{4,5} Below this temperature, liquid ^4He was found to possess remarkable flow properties as well as the “super” heat transport mentioned above. If a small test tube containing the liquid was raised above the surrounding helium bath, a mobile film would form, allowing the liquid to be transported up the inner walls, over the top and down the outer walls, eventually dripping back into the bath and thereby emptying the test tube.⁶ Furthermore, liquid ^4He could flow freely through the tiniest pores and cracks as shown by Kapitza,⁷ who performed a number of ingenious experiments involving flow properties of superfluid helium. Perhaps the most dramatic manifestation of anomalous flow behavior was the so-called fountain effect discovered by Allen and Jones.⁸ If a glass tube packed tightly with a powder such as jeweler’s rouge was partially immersed in a ^4He bath and then heated, a fountain of helium rising high above the level of the surrounding helium bath was produced. A model called the Two Fluid Model to describe these phenomena was developed by Landau⁹ and Tisza.¹⁰ According to this model, liquid ^4He below T_λ can be thought of as two interpenetrating fluids, the normal and the superfluid components. The latter component is involved in superflow through pores and cracks and does not carry entropy. Furthermore, it does not interact with the walls of a vessel containing the fluid in a dissipative fashion. Superimposed on this background superfluid component is the normal component which transports heat efficiently and exhibits viscosity, allowing transfer of energy between the liquid and the walls. This latter effect was the basis for the ingenious experiment by Andronikashvili¹¹ who actually measured the normal fluid density as a function of temperature by studying the damping of a torsional pendulum, which interacted only with the normal fluid. It was found that the normal fluid density decreased with decreasing temperature and consequently, the superfluid density increased, becoming dominant at the lowest temperatures. The normal fluid carries heat away from the heat source and is replaced by the superfluid component, so we have a countercurrent heat flow. The flow of the superfluid component toward a source of heat is spectacularly manifested in the fountain effect, mentioned above.

According to Landau the normal fluid consists of a gas of quantized thermal excitations which include the ordinary longitudinal sound waves (phonons) and short wavelength compact excitations which he named the rotons. On the basis of the two fluid model, it was predicted that heat transport would obey a wave equation which describes the compressions and rarefactions in the phonon/roton “gas”. Such a wave phenomenon was indeed discovered experimentally¹² and was named second sound.

The nature of the superfluid background still needed to be characterized. Fritz London's great contribution¹³ was to note that superfluidity could be viewed as quantum behavior on a macroscopic scale associated with the Bose-Einstein (BE) condensation. As the temperature is reduced through the transition temperature, the occupancy of the one particle ground state becomes macroscopic and can be thought of as the BE condensate. The superfluid component in the two fluid picture could be roughly identified with this condensate, although strong interactions between the atoms in the liquid modify this picture. In this scheme, the superfluid atoms are governed by a wavefunction-like entity called the order parameter, as introduced by Ginzburg and Landau¹⁴ for the case of superconductivity. The order parameter ψ for superfluid ^4He is characterized by a phase ϕ and an amplitude ψ_0 and is given by $\psi = \psi_0 e^{i\phi}$ where ψ_0 can be roughly thought of as the square root of the density of the superfluid component. The fact that the macroscopic order parameter is also described by a definite phase is called broken gauge symmetry. It has been shown that the superfluid velocity is proportional to the gradient of the phase. It is this macroscopic order parameter picture which describes how the helium atoms march in "lock-step" during superfluid flow. One beautiful consequence is the existence of quantized vortices in superfluid ^4He . This is a generalized phenomenon seen in all superfluids including superfluid ^3He and superconductivity, where a quantized current vortex must enclose a quantum of flux.

Superfluidity in liquid ^4He is thought to be a manifestation of BE condensation. What about the electrons in a superconducting metal, which obey Fermi-Dirac (FD) statistics? The theory behind superconductivity remained a mystery for about half a century. There were tantalizing clues such as the isotope effect,^{15,16} which showed that the superconducting transition temperature of a particular metal is dependent on the atomic mass of the isotope comprising that metal sample, thus connecting the superconductivity of the electrons to the dynamical behavior of the crystalline lattice of metallic ions.

The major breakthrough in our understanding of superconductivity occurred in the late 1950's when Bardeen, Cooper and Schrieffer (BCS)¹⁷ proposed their theory of superconductivity. This theory resulted in a vast revolution in the field of superconductivity. As mentioned earlier, BE particles (bosons) can congregate in their ground state at finite temperatures as a result of BE condensation. This provides the basis for the establishment of a superfluid order parameter. (The situation is really more complicated and requires that interactions be taken into account.) For a simple model involving non-interacting electrons, the conduction electrons in a metal form a sea of FD particles (fermions). At $T = 0$ all the lowest states are occupied up to the Fermi energy. Because of the Pauli exclusion principle, only one electron is allowed in each quantum state, so that macroscopic congregation in the ground state is not permissible. The BCS theory overcame this difficulty by showing that, when a metal became superconducting, the electrons in the metal formed pairs (now known as Cooper pairs),¹⁸ which had some of the properties of bosons. These pairs could thus congregate into a single ground

state (in a loose analogy to BE condensation) described by an order parameter which does not violate the Pauli principle but which leads to a conducting superfluid of electrons. The wave function describing this ground state was devised by Robert Schrieffer.¹⁷ The partners in a Cooper pair consist of two electrons whose motion is correlated even though they may be separated by distances much larger than the interparticle spacing. In other words, the pairs do not behave like Bose condensed discrete diatomic molecules. The difference may be understood in terms of modern rock and roll dancing vs. ballroom dancing, according to a marvellous analogy invented by Schrieffer and discussed by him in a number of public lectures. In ballroom dancing, the partners hold tightly to one another in analogy with diatomic molecules. The Cooper pair, on the other hand, would consist of two rock and roll dancers whose gyrations are closely related in spite of their distant separation. In between the partners of a pair, members of other pairs may pass by. The strong correlation of the pairs demonstrated by BCS leads to the pairs marching in lock step, in a fashion similar to the bosons in superfluid ⁴He.

Why do electrons form pairs? Leon Cooper¹⁸ in fact showed that at low enough temperatures electrons form pairs as long as there is a *net* attractive force, even a very weak one. We know that the electrons all have negative charges which result in strong Coulomb repulsion but this can be balanced out and even reversed by the dynamic response to the electrons of the positive ions forming a crystal. The results of the isotope effect experiments mentioned earlier provided the key to this insight. As an electron moves through the lattice it attracts the positive ions, forming a region with a higher density of positive ions, which can in turn *attract* other electrons. This role of the massive positive ions explains the isotope effect. The density fluctuations of the ions that are associated with the passage of an electron can be described in terms of quantized lattice waves called phonons, and the attraction is thus associated with electron-phonon interactions.

The temperature T_c at which a metal becomes superconducting is the temperature for which it becomes energetically favorable to form pairs. The temperature T_c is typically 1000 times smaller than the Fermi degeneracy temperature T_F , where the thermal de Broglie wavelength becomes comparable to the mean interparticle spacing a_0 and quantum effects become important. Pairing superfluidity in Fermi fluids is therefore much more difficult to achieve, in contrast to the case for bosons where the onset of superfluidity occurs when the quantum fluid condition $\lambda_T \gtrsim a_0$ is satisfied. For the case of pairing superfluidity, two electrons near the Fermi surface can give up energy by forming a Cooper pair. The same energy, say 2Δ , must be supplied to break up a Cooper pair. The size of this energy gap 2Δ is a fundamental parameter in the theory of superconductivity. The energy gap parameter Δ approaches zero as we approach T_c but Δ grows in size as a superconductor is cooled to absolute zero. Why should the energy gap be a function of temperature? We take the mean field or molecular field view which is so successful in explaining magnetism. For that case, the tendency toward further ordering increases with increasing ordering, which corresponds to a strengthening of

the molecular field. Applying this to the case of pairing in a superconductor, we find that a larger number of pair states leads to a larger binding. The energy gap is a measure of the binding energy of a pair and will therefore increase as the number of pairs increases with decreasing temperature. This behavior is fully accounted for by the BCS theory.

Many years before the BCS theory, Fritz and Heinz London¹⁹ had developed phenomenological equations for superconducting metals. Fritz London²⁰ showed how these equations could be discussed in terms of his idea of quantum mechanics on a macroscopic scale. In 1950 Ginzburg and Landau¹⁴ proposed a complex order parameter ψ , consistent with London's discussion, representing the many electron state in a superconductor, where $|\psi|^2$ was equal to the local density of superconducting electrons. Here we have invoked the two fluid model familiar from our discussion of superfluid ^4He , where we now consider two interpenetrating electron fluids corresponding to normal and superconducting components. (We have already mentioned a Ginzburg Landau order parameter for superfluid ^4He .) Ginzburg and Landau derived a differential equation from an expansion of the free energy in powers of ψ given by

$$\frac{1}{2m^*} \left(\frac{\hbar}{i} \nabla - \frac{e^*}{c} \vec{A} \right)^2 \psi + \beta |\psi|^2 \psi = -\alpha(T) \psi.$$

This equation resembles the Schrödinger equation but has an additional term in $|\psi|^2$. Although it is not the Schrödinger equation, the electric current obtained from this equation has exactly the same form as that for a wave function, namely

$$\vec{J} = \frac{e^* \hbar}{2m^* i} (\psi^* \nabla \psi - \psi \nabla \psi^*) - \frac{(e^*)^2}{m^* c} |\psi|^2 \vec{A}.$$

Experiments later showed that $e^* = 2e$ and $m^* = 2m$, thus making contact with the BCS theory of superconductivity in metals and showing that the order parameter describes the correlated pairs.^{21,22}

The order parameter is again given by the simple expression $\psi = \psi_0 e^{i\phi}$ which possesses a phase ϕ and an amplitude ψ_0 which increases in magnitude with the gap parameter Δ . We have already interpreted $|\psi|^2 = \psi_0^2$ in terms of the two fluid model, so the amplitude ψ_0 is simply the square root of the density of superconducting electrons. As in the case for superfluid ^4He , the phase of the order parameter is of paramount importance for the superflow properties. Such phenomena as quantized flux^{21,22} and the Josephson effect²³ (corresponding to the tunneling of pairs) require phase coherence throughout the superconductor.

Could the pairing theory be applied to other systems? Liquid ^3He was the most obvious candidate to be examined. It is composed of neutral atoms with a nuclear spin angular momentum of $\hbar/2$ and a nuclear magnetic moment. The ^3He atom has an odd number of elementary particles and so it obeys FD statistics and the Pauli exclusion principle. The atoms in the liquid are known

to interact strongly so one cannot strictly apply the theory of an ideal Fermi gas to predict the properties of liquid ^3He in the normal non-superfluid Fermi liquid (NFL), meaning the liquid above any possible superfluid transition temperature. Lev Landau²⁴ formulated a theory of strongly interacting Fermi liquids which introduced the idea of quasiparticles corresponding to bare fermions “clothed” by their interactions with the others. The various properties of normal liquid ^3He qualitatively resembled the properties of ideal Fermi gases, but the numerical factors were entirely different. The Landau theory showed how these properties could be expressed in terms of a set of parameters called the Fermi liquid parameters. In a Fermi liquid at low temperatures, the thermally excited quasiparticles will occur in a narrow band near the Fermi surface with energy width of order kT . Only the quasiparticles in this narrow band of states can participate in scattering or in thermal excitations. As T is lowered the width of the band shrinks and fewer quasiparticles can participate in such events. As a result the specific heat and the entropy depend linearly on temperature ($c = \gamma T$) and the mean free path is proportional to T^{-2} . The thermal conductivity therefore has a $1/T$ dependence and the viscosity has a $1/T^2$ dependence. The numerical constants for an interacting Fermi fluid will differ from those for an ideal Fermi gas due to interactions described by Landau parameters, as discussed above. These and other experimental properties of normal liquid ^3He were studied in laboratories around the world, but the dominant group was led by John Wheatley,²⁵ first at the University of Illinois and then at the University of California at San Diego (La Jolla). A primary result of these investigations was the evaluation of the Landau Fermi liquid parameters. The Landau theory also made an important prediction; collisionless sound, called by Landau zero sound.²⁴ Ordinary sound in a gas for example involves the propagation of waves of compression and rarefaction in a state of local thermodynamic equilibrium brought about by collisions between the molecules. At the lowest temperatures in a Fermi liquid the collisions are substantially absent and ordinary sound dies away. According to Landau, a new mode of sound propagation arises at the lowest temperatures involving self-consistent rearrangements of the quasiparticles under the influence of Fermi liquid interactions. This prediction was dramatically confirmed in laboratory experiments by Keen, Matthews and Wilks,²⁶ and Abel, Anderson and Wheatley.²⁷

Because of the strong interactions between ^3He atoms, it was soon realized that if Cooper pairs formed in liquid ^3He , they would be quite different in nature from the pairs associated with superconducting electrons. In ordinary superconductors, the Cooper pairs have zero orbital angular momentum ($l = 0$) so the members of a pair do not rotate around one another. The strong short range repulsion of the quasiparticles in liquid ^3He prevents this type of pairing from occurring, but higher angular momentum pairing is indeed possible, as was first proposed by Lev Pitaevskii.²⁸

Over the years a number of higher orbital angular momentum pairing states were proposed for a hypothetical superfluid state of liquid ^3He . Both p wave ($l = 1$) and d wave ($l = 2$) states of relative orbital angular momentum

were suggested. Among the early studies were those by Emery and Sessler²⁹ and Anderson and Morel.³⁰ The proposals for p wave pairing by Balian and Werthamer,³¹ and Anderson and Morel³⁰ were later identified with the *actual* superfluid phases of liquid ^3He .

An important feature of odd l pairing is that it requires the total spin of the pair to be 1 (not zero as in even l pairing). Thus any order parameter representing odd l pairing will possess the internal degrees of freedom associated with non-zero spin and orbital angular momentum. This fact is of the utmost importance for understanding the properties of superfluid ^3He , and contrasts dramatically to ordinary superconductivity for which $S = L = 0$.

It is extremely difficult to calculate the transition temperature to a superfluid phase of liquid ^3He . Such an estimate depends very sensitively on the detailed nature of the interactions between the ^3He quasiparticles. Since there is no external crystal lattice to mediate these interactions, the pairing mechanism itself must be *intrinsic*. Layzer and Fay³² considered the fact that the nuclear magnetic susceptibility of liquid ^3He was considerably higher than would be expected for an ideal FD gas of comparable density. This result indicated that there was at least some tendency for the liquid to be ferromagnetic. They considered a pairing mechanism based on spin fluctuations which goes something like this: As a ^3He quasiparticle passes through the liquid it tends to polarize spins of neighboring quasiparticles parallel to its own spin because of this ferromagnetic tendency. Another ^3He quasiparticle approaching this polarized cloud will be attracted to the cloud if its spin is parallel to that of the cloud and the original quasiparticle. Thus it becomes favorable to form Cooper pairs with non-zero spin which requires odd orbital angular momentum via the Pauli Exclusion Principle.

The most striking characteristics, then, of the hypothetical superfluid ^3He were that (1) it would need to have an intrinsic pairing mechanism not mediated by an ionic lattice for example and (2) the resulting Cooper pairs would probably have internal degrees of freedom. These two properties would distinguish superfluid ^3He from the other known superfluids, superfluid ^4He and superconducting electrons.

In spite of considerable progress on the theoretical front, before 1971 no evidence of a superfluid transition had been found by experimenters who were pushing the cooling technology to lower and lower temperatures. Experimentalists and theorists alike became dubious that the Holy Grail would be found in a reasonable temperature range. A mood of gloom and pessimism prevailed by about 1970.

EVENTS LEADING TO THE DISCOVERY OF SUPERFLUID ^3He : A PERSONAL ACCOUNT

The rare isotope of helium, ^3He , first became available for research in low temperature physics after World War II as a byproduct of the nuclear weapons program. It was obtained from the radioactive decay of tritium which decays via beta decay with a twelve year half life to ^3He . Some of the earliest research

on liquid ^3He was performed³³ at the national laboratories which were involved in nuclear weapons research. My Ph.D. thesis adviser Professor Henry A. Fairbank at Yale University was one of the pioneers in research involving ^3He . In his early work he specialized in studies of second sound in liquid ^3He - ^4He mixtures. In the autumn of 1955, I had the good fortune to be selected as the first graduate student to investigate pure liquid ^3He . My first project was to study the thermal conductivity of liquid ^3He with the idea of searching for Fermi-Dirac degeneracy effects which would lead to a $\kappa \sim 1/T$ dependence at low temperatures. It was anticipated that the thermal conductivity of this liquid would be very small at temperatures below the liquefaction temperature of 3.2 K as is the case for liquid ^4He above the superfluid transition. The experimental set up was as simple as could be imagined. The liquid was contained in a thin-walled cupro-nickel tube which had a very small thermal conductivity, thus limiting the amount of heat transport through this tube. (Nevertheless, it was necessary to correct for this as well as the thermal boundary resistance between solid walls and the liquid.) Simple (semi-conducting) carbon resistors served as the thermometers. At the top of the tube was an electrical heating coil and at the bottom a heat sink consisting of a copper block attached to a paramagnetic salt which was used to cool the sample to 0.2 K or less by adiabatic demagnetization. The magnetic susceptibility of this salt, measured with a ballistic galvanometer, served as the primary thermometer and was used to calibrate the carbon resistance thermometers. The thermal conductivity was determined from the standard formula $\dot{Q} = \kappa A \Delta T / \Delta X$ with corrections for added heat flow through the cupro-nickel tube. Measurements of the resistance thermometers were accomplished with a home-made A.C. resistance bridge including a phase sensitive detector and a tuned amplifier to assure great sensitivity and low noise even when the voltages across the thermometers were small enough to prevent significant self heating.

The initial results of the experiment were not very interesting; the thermal conductivity simply continued to decrease as the temperature decreased in very much the same fashion as that of liquid ^4He above the superfluid transition, with no evidence of Fermi-Dirac statistics. Nevertheless, when the experiments were run at higher powers, a very intriguing thing happened. Below a certain temperature, T_m (~ 0.5 K), the heat conduction rapidly increased as the temperature was lowered further. This effect was attributed to convective heat flow, the onset of which corresponded to a maximum in the density. To verify this, an inverted cell was constructed with the heat flowing upward. For this new geometry, the convective heat flow appeared above T_m , as would be expected if a density maximum occurred at T_m . There was wonderful serendipity here. We were studying thermal conductivity but the most interesting result involved the density.³⁴

The existence of a density maximum at T_m implied that for temperatures less than T_m , the thermal expansion coefficient was *negative* and via a Maxwell relation

$$\left(\frac{\partial V}{\partial T}\right)_P = -\left(\frac{\partial S}{\partial P}\right)_T$$

it was evident that the entropy should increase with pressure below T_m . The entropy is a very basic property which could be used to estimate the interactions between the ^3He particles and so we decided to measure the density directly by measuring the dielectric constant, which for helium is related to the density via the Clausius-Mossotti relation,

$$\frac{\epsilon - 1}{\epsilon + 2} \frac{M}{\rho} = \frac{4\pi}{3} A$$

where A is the atomic polarizability and M is the atomic mass.

The method chosen to measure ϵ was to employ a stable radiofrequency oscillator with a tank circuit whose capacitor contained the sample. The frequency varied as the temperature was changed and the dielectric constant of the liquid ^3He changed. A great deal of mechanical stability was required since the electronic circuitry involved vacuum tubes which were at room temperature, while the capacitor and inductor forming the tank circuit were at the bottom of the cryostat, a full meter away. With the apparatus a series of measurements was carried out over a range of temperatures and pressures which clearly showed the density maximum and enabled the entropy of compression to be obtained from the measured thermal expansion coefficients.³⁵

At the time these experiments were being performed, there was a great deal of interest in determining the melting curve of ^3He . Because the nuclear moments are very small, it was expected that solid ^3He would undergo nuclear magnetic ordering only at very low temperatures (This nuclear magnetic ordering transition was later discovered³⁶ at about 1 mK by my Cornell colleague and fellow laureate Robert C. Richardson, his student William Halperin, and their associates). Therefore in the range of temperatures above 0.01 K, the nuclear spins of the ^3He atoms comprising the solid should be almost fully disordered. For spin 1/2 nuclei this required that the entropy S should be equal to $R \ln 2$ per mole.

On the other hand liquid ^3He obeys Fermi-Dirac statistics. The departure from classical behavior occurs roughly at the temperature where the thermal de Broglie wavelength is on the order of the mean interparticle spacing. This temperature is of order 1 K for liquid ^3He (depending on the density). Well below this temperature (called the Fermi degeneracy temperature T_F), the specific heat and the entropy will both be linear functions of the absolute temperature, i.e. $S = \gamma T$. Let us now consider the implications of the above discussion to the liquid-solid phase equilibrium which is determined by the famous Clausius-Clapeyron equation. According to this equation the slope of the melting curve is given by

$$\frac{dP}{dT} = \frac{S_{\text{liquid}} - S_{\text{solid}}}{V_{\text{liquid}} - V_{\text{solid}}} = \frac{\text{Latent Heat}}{T(V_{\text{liquid}} - V_{\text{solid}})}.$$

For ^3He , V_{liquid} is always greater than V_{solid} , so the denominator is always positive. On the other hand, the numerator will *change sign* as one cools into the Fermi degenerate region because $S_{\text{liquid}} = \gamma T$ will become less than the constant solid entropy $S_{\text{solid}} = R \ln 2$ corresponding to random spin orientation, so at the lowest temperatures the slope of the melting curve becomes *negative*. Furthermore, in this regime, the latent heat becomes negative, i.e. *it takes heat to freeze liquid ^3He* . At the higher temperatures, the entropy of the liquid will be greater than $R \ln 2$ per mole so that the melting curve will have a minimum. Idealized melting and entropy curves are shown schematically in Figure 1. Because the density of the solid is about 5 % higher than that of the liquid, it was possible to discern the presence of solid in our dielectric constant cell. Above the temperature of the minimum, solid could easily be formed in the cell as the pressure in the capillary tube connecting the ^3He pressurizing system at room temperature to the cell was increased. Below the temperature of the minimum, T_{min} , the capillary between the cell and room temperature became blocked as the pressure was increased and so no solid could be admitted into the cell. This difference in behavior above and below T_{min} allowed the temperature and the pressure of the minimum to be obtained. The best values of pressure and temperature as of 1996 for this minimum are 29.3 bar and 0.32 K respectively.

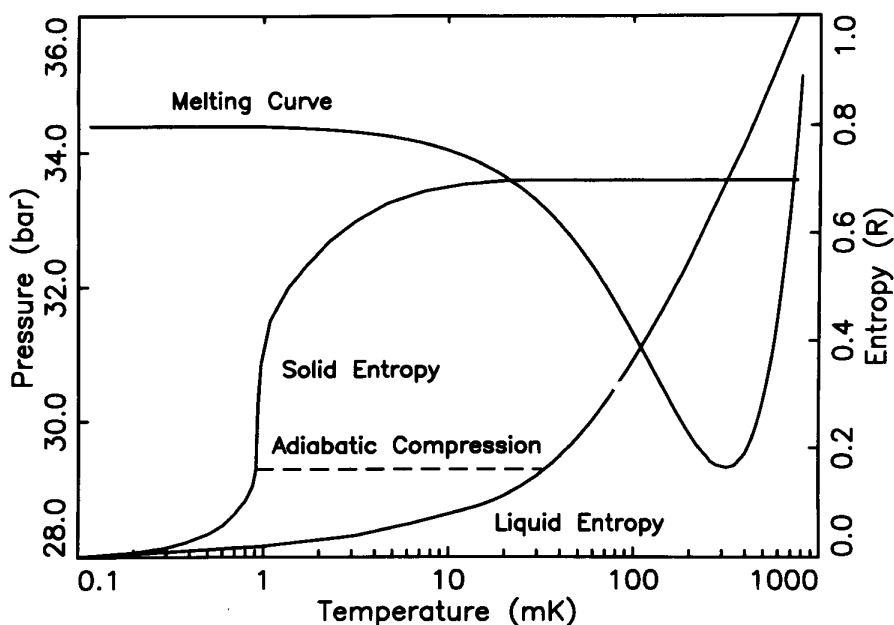


Figure 1. A semilog plot of the melting pressure of ^3He versus temperature showing the minimum at 0.32 K and 29.3 bar. An idealized semilog plot of the entropy of liquid ^3He and the entropy of solid ^3He at the melting curve is shown on the same graph. For the highest temperatures, the liquid entropy was calculated from the melting curve via the Clausius Clapeyron equation and the assumption that $S_{\text{solid}} = R \ln 2$. The two entropy curves cross at the melting curve minimum. The steep slope of the solid entropy curve near 1 mK corresponds to a magnetic phase transition in the solid. The dashed line is the path of an adiabatic compression from liquid to solid (Pomeranchuk cooling), to be discussed later.

The blocked capillary made extremely difficult any measurement near or along the melting curve which required a variation of the pressure or even a knowledge of the pressure for $T < 0.32\text{ K}$ and $P > 29.3\text{ bar}$. This included the possibility of carrying out a suggestion by the Russian particle theorist, Isaac Pomeranchuk³⁷ that one could cool ^3He by pressurizing the liquid to form solid ^3He at temperatures below T_{\min} . My Ph.D. thesis advisor, Henry Fairbank, first told me about Pomeranchuk's idea shortly before I left Yale for Cornell University as a newly minted Ph.D. in January 1959. He said that it would be a wonderful thing if I could invent a method for carrying out Pomeranchuk's suggestion in the laboratory. His enthusiasm was quite compelling, and I would often dream about Pomeranchuk cooling after moving to Cornell.

My first mission in 1959 as a young faculty member at Cornell was to convert an empty room into a low temperature laboratory capable of investigating liquid ^3He in the temperature region below 1 K. The most crucial task was to write a research proposal to the National Science Foundation to obtain funding to build up the laboratory and provide for graduate students to help in the research program. One of the major pieces of equipment required was an electromagnet for adiabatic demagnetization with sufficient field homogeneity for nuclear magnetic resonance (NMR) studies. Fortunately we were successful in obtaining a National Science Foundation grant which enabled us to begin taking measurements in 1960. The earliest experiments involved studies of nuclear magnetic resonance along the melting curve of ^3He . Later studies involved experiments on the melting and freezing properties of ^3He - ^4He mixtures. These latter measurements made use of commercial strain gauges to determine the pressure of the sample in regions where the fill capillary was blocked. Development of a much more sensitive strain gauge was underway which utilized a stable tunnel diode oscillator to drive a tank circuit, one of whose capacitor plates was the flexible wall of the cell which thus formed the pressure sensor. Cell pressure changes would be registered as frequency changes of the oscillator. The standard modern design for pressure transducers as developed by Straty and Adams³⁸ is similar in principle. Nowadays, sensitive capacitance bridges are used in conjunction with these gauges. Unfortunately all of these experiments were interrupted when the entire laboratory began to collapse into the excavation for a new physics building (now Clark Hall). By good luck all of the equipment was saved before the laboratory was totally destroyed. A temporary laboratory was constructed in the metallurgy building where experiments were performed to finish mapping out the complete phase diagram of the melting and freezing properties of ^3He - ^4He mixtures³⁹ and to make the first observation of transverse sound in solid ^4He .⁴⁰

During this period, I began to think seriously about the possibility of performing Pomeranchuk cooling experiments after we finally moved into the new physics building. We have previously discussed the fact that pressurizing through the minimum in the melting curve resulted in a fill capillary blocked with solid. Therefore, to pressurize the sample along the melting curve at

temperatures below the melting curve minimum, some external force had to be applied to the ^3He , independent of any external pressure communication through the fill capillary. We thought at the time that the best way to do this would be to construct a Pomeranchuk cell from a flexible thin-walled bellows. One could immerse the Pomeranchuk cell in liquid ^4He and raise the pressure of the liquid to 25 atmospheres pressure before solidification of the ^4He would occur. This was still less than the pressures of 29–34 atmospheres required to compress ^3He to pressures above the pressure of the melting curve minimum. An extra boost needed to be applied to attain the requisite pressure. The idea which we had at the time was to add an external spring to provide this extra force. A bellows and spring combination had been used previously by Grilly *et al.*⁴¹ to study the properties of liquid ^3He near the melting curve minimum. (If properly placed, the spring would not contribute substantially to the heating of the ^3He sample). This provided the basis for our further thinking although as time went on there were many substantial improvements and modifications that went well beyond this early scheme.

The academic year 1966–67, my sabbatical year, was spent at the Brookhaven National Laboratory. There I had the time to interact strongly with Paul Craig, Thomas Kitchens, Myron Strongin, and Victor Emery. They and other staff members at Brookhaven made many extremely valuable suggestions and were helpful in many other ways. For example, one of the objections to Pomeranchuk cooling was the fact that the stretching of metal parts would lead to internal frictional heating, which would counter the cooling effect of compressing liquid ^3He into the solid phase. Discussions at Brookhaven convinced me that this problem could be overcome with careful design. Less work would be done and smaller energy losses could be achieved with a thinner and more flexible bellows. Basically, however, it was really an article of faith that Pomeranchuk cooling could be brought to fruition.

At a Solid State Sciences Panel meeting in the mid-1960's Philip W. Anderson and John C. Wheatley suggested that there was a great frontier opening up in ultra low temperature physics. This vision of the future by two such distinguished scientists greatly enhanced the prospects for our obtaining a higher level of research support. This allowed us to hire my colleague Robert C. Richardson as a research associate under a university-wide grant to the Cornell Materials Science Center by the Advanced Research Projects Agency. Bob had been a graduate student of Professor Horst Meyer at Duke University. Not only was he an expert on nuclear magnetic resonance (NMR) in solid ^3He and cryogenics but he also had exceptional vigor and scientific judgment. All of these skills and traits would be of the utmost importance to our low temperature program at Cornell. Within a short time, Bob became a member of our faculty. Shortly before Bob's arrival at Cornell, John Reppy had also joined our faculty. John's main area of expertise was experimental superfluid ^4He . We benefitted tremendously from his friendship, his wisdom, his sage advice and his extraordinary technical ingenuity.

The development of the ^3He – ^4He dilution refrigerator in the mid-60's⁴² and later improvements⁴³ had an enormous impact on ultra-low temperatu-

re physics. It had now become possible to continuously cool experimental samples to temperatures of order 10 mK. Previously, adiabatic demagnetization of paramagnetic salts was the only way to cool to this temperature range. Typically, a paramagnetic salt and the sample were cooled to the base temperature and then warmed slowly, a "one shot" experiment. Continuous adiabatic demagnetization refrigerators could be built but they were exceedingly cumbersome. The decision was therefore made to develop a dilution refrigerator system at Cornell. This effort was spearheaded by Bob Richardson. Our program was aided by very able new graduate students, James R. Sites, Linton Corruccini and Douglas D. Osheroff. The dilution refrigerator was to serve as a 10 mK low temperature platform from which to launch Pomeranchuk cooling.

The first Cornell Pomeranchuk cell was based on a brilliant but complex design involving two sets of thin, very flexible nested bellows suggested by John Reppy to minimize the effects of internal frictional heating in the metal bellows and to utilize a hydraulic press method for obtaining a mechanical advantage. It was first used successfully in the thesis experiment of Jim Sites who performed NMR susceptibility measurements on solid formed in the cell during compression. The purpose of the experiment was to study Curie-Weiss behavior as a precursor to the anticipated magnetic phase transition in solid ^3He . A Physical Review Letter on this experiment was published by Sites, Osheroff, Richardson and Lee.⁴⁴ Temperatures of about 2 mK were achieved. It was suspected that the lowest temperature that could be attained was limited by heating caused by solid being crushed in the bellows convolutions.

In the meantime, other laboratories were not standing still. Unbeknownst to us, Yuri Anufriyev at the Institute for Physical Problems (now the Kapitza Institute) in Moscow was the first to actually achieve Pomeranchuk cooling in 1965.⁴⁵ His cell was based on a stressed diaphragm technique in which the ^3He was forced into a cell with strong but flexible walls until the inlet capillary was blocked at high pressures. For this case, the flexible walls played the role of the spring mentioned in our earlier discussion. In the actual design, the flexible walled tube was placed inside a larger rigid tube. The outer annular space contained the ^3He . Liquid ^4He in the inner tube was then pressurized to pressures approaching the melting pressure of ^4He . In spite of the stress applied to the walls of the ^3He cell to achieve the necessary volume change (5 %) for solidification, internal frictional heating did not seem to be a serious limiting factor. Later on John Wheatley and his associates modified the Anufriyev design somewhat and also were able to achieve Pomeranchuk cooling.⁴⁶ On the basis of these developments, several of us at Cornell realized that if the stressed diaphragm cells could achieve substantial Pomeranchuk cooling, it was no longer necessary to worry so much about internal frictional heating. Thus stronger bellows could be used in the design of any future Cornell Pomeranchuk cell.

An important consideration in the design of a Pomeranchuk experiment was the thermal isolation between the Pomeranchuk cell and the dilution refrigerator once the compressional cooling process was in operation. Fortun-

ately the thermal boundary resistance between liquid ^3He and any metal heat link to the dilution refrigerator is quite large, which severely limits heat flow between the ^3He in the cell and the dilution refrigerator mixing chamber. Therefore the heat flow is very slow, or in the words of the late John Wheatley,⁴⁷ "Time is the thermal switch." In all of the early Cornell Pomeranchuk cells, even though the cells were bolted directly to the dilution refrigerator mixing chambers, many hours of experimentation below 3 mK were made available.

A BRIEF ACCOUNT OF THE DISCOVERY

It was clear from the outset that Douglas Osheroff was an extremely promising graduate student with tremendous potential. Once Jim Sites had obtained his Ph.D., Doug was next in line to take on the role as the lead graduate student in the Pomeranchuk cooling program. A great deal had been learned about Pomeranchuk cooling experiments as a result of work performed at Cornell and elsewhere. We knew that we had a powerful cooling technique which could cool a mixture of solid and liquid ^3He along the melting curve to temperatures of 2 mK or lower. Since we wanted to study ^3He , the cooling method had the advantage that the sample *was* the refrigerant, so that awkward heat transfer between sample and refrigerant could be avoided. The disadvantage was that the sample was confined to the melting curve so liquid and solid ^3He were simultaneously present in the cell.

With Doug Osheroff and Bob Richardson on board, it was time to start considering the next generation of Pomeranchuk cells to continue our program of cooling ^3He with the goal of searching for the long anticipated magnetic transition in solid ^3He . A number of ideas were considered including the rather whimsical suggestion of using a weight made of a heavy metal such as gold at the top of the flexible bellows which would supply the extra force needed to make up the difference between the melting pressure of ^4He and that of ^3He . There were no springs, stiff bellows or cell walls to be heated and the bellows could be very pliable. Certainly there would be no heating involving the gravitational field. Furthermore, the price of gold was rising rapidly at the time, so at the end of the experiment the gold weight could be sold to help support the research program!

We settled on a cell design which Doug Osheroff developed while he was recovering from a skiing-induced knee injury. This cell, shown in Figure 2 made good use of many of the lessons learned in previous work at Cornell and elsewhere. It employed two beryllium-copper bellows connected by a piston rod to transmit the force to pressurize the ^3He sample. The cross sectional area of the ^4He bellows was larger than that of the ^3He bellows, leading to a pressure amplification, as in a hydraulic press. When liquid ^4He in the upper bellows was externally pressurized, it forced the piston rod down, causing the lower bellows to distend downward into the ^3He cell. The opening up of the lower bellows prevented solid ^3He from being trapped and squeezed in the convolutions. Bob Richardson was very eager to have the most sensitive

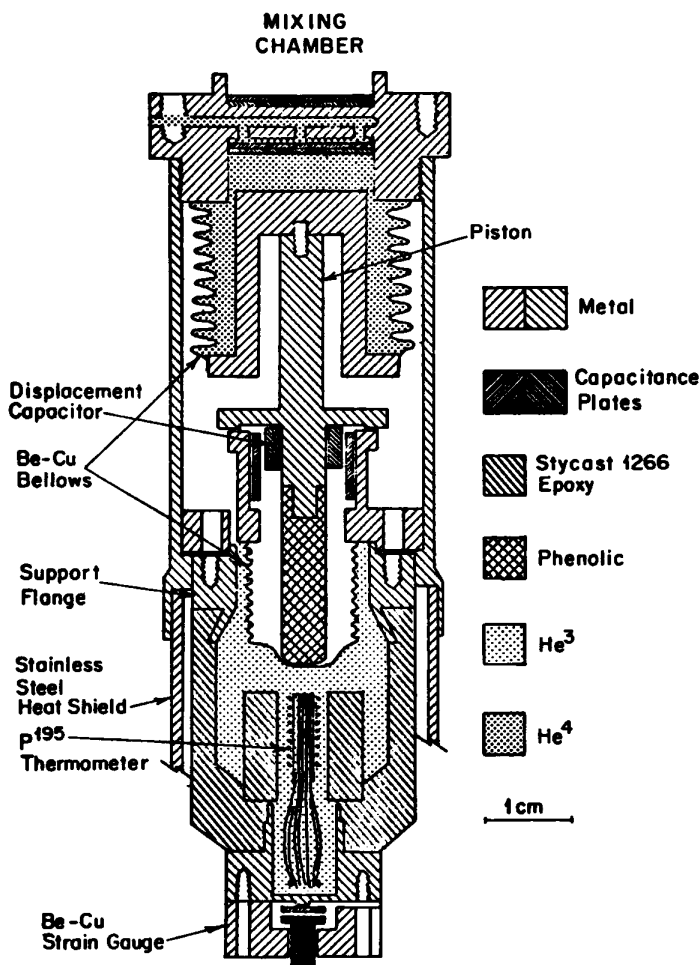


Figure 2. The Pomeranchuk cell used in the discovery experiments of Osheroff, Richardson and Lee. The pressure applied to the liquid ^4He in the upper bellows causes a piston rod to drive the lower bellows into the ^3He cell to increase the ^3He pressure. The ^4He bellows is larger than the ^3He bellows, thus providing a favorable compression ratio, in analogy to a hydraulic press.

melting pressure gauge possible. Therefore a sensitive capacitance strain gauge of the Straty-Adams³⁸ design was attached to the bottom of the cell containing the ^3He , allowing the ^3He pressure to be monitored during the compression process, thus providing a secondary melting curve thermometer. A platinum NMR thermometer which made use of a coil wrapped around a bundle of fine Pt wires (or copper wires in the first experiments) served as the primary thermometer down to 3 mK, below which it tended to lose thermal contact with the sample, possibly as a result of solid formation around the wires. In spite of the lack of a primary thermometer below 3 mK it was possible to obtain an estimate from melting pressure measurements of the temperature by extrapolating the melting curve. It was also possible to monitor the melting pressure as a function of time as the cell volume was changed at a constant rate. It was exactly this procedure which enabled Doug Osheroff to

observe some peculiar but highly reproducible features on a chart recorder plot of the melting pressure vs. time in late November 1971.

I was heavily involved in preparing lectures for one of our large courses and did not find out about the observations immediately. When I did find out I was very excited. In fact all three of us were in a state of euphoria and knew we were on the brink of a major discovery. This was really the first defining moment in the experiment. A typical plot of the pressure vs. time observations for a complete cooling and warming cycle is shown in Figure 3. Anomalies labeled *A* and *B* in this figure were observed on cooling and corresponding features *A'* and *B'* were observed on warming. It certainly appeared that these effects were associated with new phase transitions, but *were they in the liquid or the solid?* The flattening in the pressure trace at *B'*, corresponding to a brief hesitation in the warming, was a rather subtle feature which was not observed until several days after the initial observation of the signatures *A*, *A'*, *B*. I clearly recall coming in to the laboratory to lament to Doug that we had not as yet seen the signature for *B'* corresponding to the warming analog to *B*. At that very moment the chart recorder was beginning to display a small feature which was the first evidence for *B'*. The brief flattening was interpreted as a manifestation of latent heat associated with a first-order transition. Giving this idea further credence were the peculiar zig-zags seen at *B* which could be a characteristic of a supercooled transition where the latent heat was suddenly released, giving a brief rapid warming. Supporting the supercooling inter-

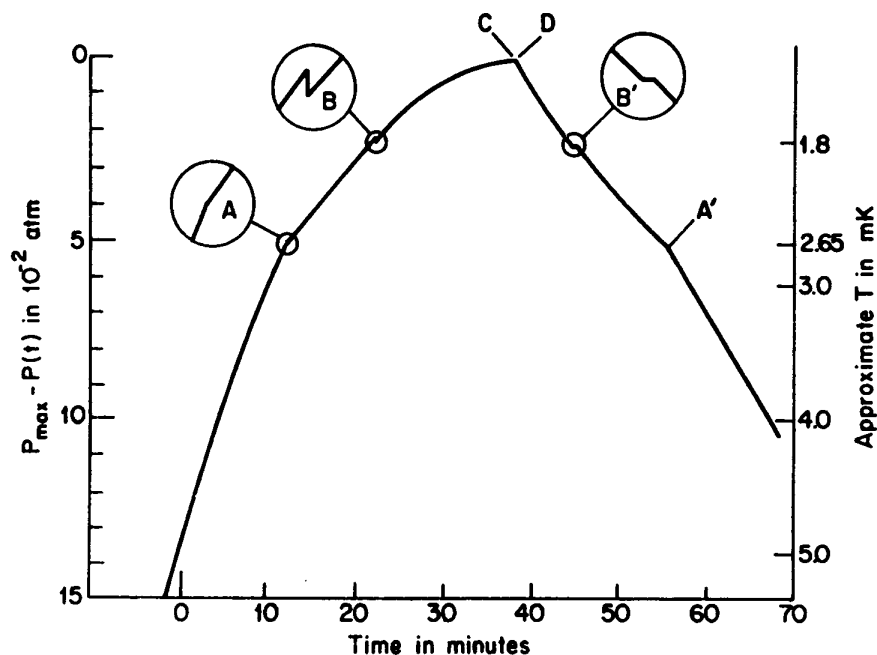


Figure 3. Features observed on a plot of cell pressure vs. time during compressional cooling to the minimum temperature followed by warming the cell during decompression. The *A* and *A'* features were changes in slope. They always occurred at precisely the same pressure. Lower temperature features *B* and *B'* were also observed. On cooling through *B* a sudden pressure drop appeared, and on warming through *B'* a small plateau was observed. The pressure at *B* was always greater than or equal to the pressure at *B'*.

pretation was the fact that B' was reproducible whereas B occurred at a pressure that was not reproducible but was always greater than the pressure corresponding to B' . The features A and A' , corresponding to slope changes on the pressure-time traces, were completely reproducible, showing no signs of supercooling. Although our thermometry was crude, we were able to estimate the temperature of the A transition, $T_{A'}$ to be about 2.7 mK and the temperature of the B' transition, $T_{B'}$ to be about 2.1 mK, based on the temperature scale in use in 1971.

Since both liquid and solid ^3He were present in the cell, we at first thought that the A transition corresponded to the long sought second order magnetic phase transition in solid ^3He . Possibly the variation of the specific heat of solid ^3He with temperature near such a phase transition could have given a signature similar to that observed in the melting pressure traces. The rapid response of the sample upon passing through the supercooled B transition was much more difficult to interpret in terms of a phase transition in solid ^3He . Nevertheless, our first paper, published in Physical Review Letters, was entitled "Evidence for a New Phase of Solid ^3He ."⁴⁸ John Goodkind of the University of California San Diego in a private conversation with me at an American Physical Society meeting indicated that he was quite sure the action was taking place in the liquid, not the solid. We also received a letter from Victor Vvedenskii at the Institute for Physical Problems (now the Kapitza institute) in Moscow suggesting that the behavior at the A feature was associated with a step in the specific heat corresponding to a pairing transition in liquid ^3He in analogy with a similar specific heat step seen at the superconducting transition in metals.

The overall research plan from the beginning was to perform NMR studies in the cell. This became even more urgent because of the need to unambiguously establish the identity of the A and B features. The results of these NMR studies were to give, as is discussed below, a clear indication that both the A and B transitions were associated with *liquid* ^3He !

Since both liquid and solid were present in the cell, some means was required to distinguish between the liquid and the solid. Solid ^3He exhibits Curie-Weiss behavior at low temperatures and so its magnetic susceptibility is large, since all of the spins participate. On the other hand liquid ^3He obeys FD statistics, and so its magnetic susceptibility is governed by Pauli paramagnetism which requires that only those quasiparticles in the immediate vicinity of the Fermi surface are free to flip. Thus the liquid susceptibility must be very small, since only a small fraction of the spins are involved in a magnetic response.

If a field gradient is superposed on the homogeneous applied steady field, the Larmor frequency $\omega = \gamma H$ will vary across the cell. Thus different regions of the cell have different Larmor frequencies, so that the NMR response of each of the small regions will have to correspond to a different frequency. Sweeping the frequency or the magnetic field enabled us to monitor different regions of the cell. This was one of the first applications of magnetic resonance imaging (MRI) which is now an essential tool in medical diagnosis.⁴⁹

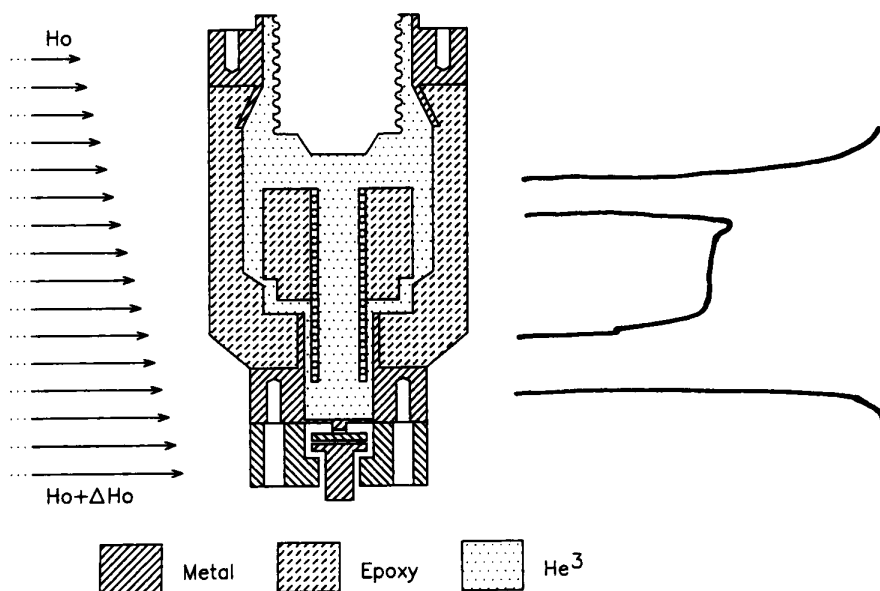


Figure 4. The lower portion of the Pomeranchuk cell of Figure 2 showing an NMR coil along the cell axis. A small field gradient was applied to the cell as shown by the arrows, providing for one dimensional magnetic resonance imaging. An idealized plot of the ^3He susceptibility vs. height is shown on the right. The solid, corresponding to the large susceptibility peaks, tends to clump at the ends, allowing the center of the coil to be relatively free of solid.

A radiofrequency coil was introduced into the ^3He cell as shown in Figure 4. The gradient in the applied dc magnetic field is indicated by the arrows. It was very fortunate in these experiments that the solid formed in localized regions of the cell. Thus it was possible to separately examine the behavior of the liquid corresponding to a small susceptibility and the solid corresponding to a large susceptibility as shown in Figure 5. As the sample cooled through B , the *liquid* susceptibility suddenly dropped by about a factor of two. Upon making this observation, Doug called me at home in the early hours of the morning. I was elated when I heard the news! It was clear that the B phase was a liquid phase. Furthermore, the susceptibility drop could perhaps be related to a BCS pairing transition. This was the second defining moment in the ex-

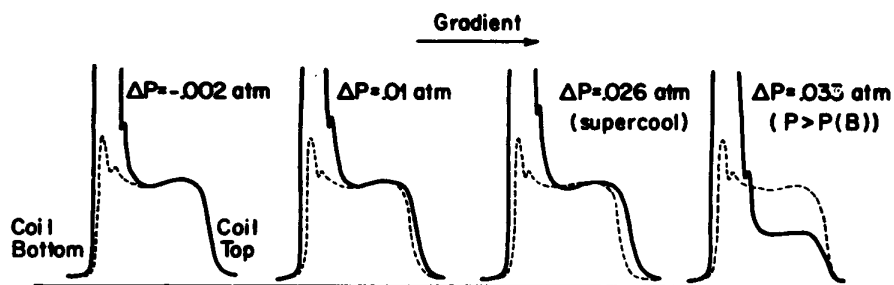


Figure 5. A sequence of NMR profiles taken with a field gradient in the cell of Figure 4, as the ^3He sample is cooled along the melting curve. We show a run for which solid happened to form at only one end of the coil. The susceptibility associated with the liquid drops abruptly as we cool through point B .

periment. At this point I vowed to myself that I would be present at any other such moment.

Since I believed that it was important to check for any possible frequency shift, I asked Doug to remove the field gradient in order to examine the response of the mixture of the liquid and solid in a homogeneous field. As the three of us watched, a truly dramatic thing happened when the sample was cooled into the *A* phase. At the *A* transition a satellite line emerged from the main mostly solid peak and steadily moved to higher frequencies as the sample cooled. At the *B* transition this satellite line abruptly disappeared back into the main peak, so that the *B* phase did not show a frequency shift away from the Larmor frequency. These effects are illustrated in Figure 6. This was the third defining moment in the experiment. The satellite line had the same amplitude and shape as the all liquid line in the normal Fermi liquid phase when no solid was present in the cell. Furthermore, the amplitude did not change with temperature. Thus the satellite line corresponded to the entire liquid line shifting in frequency as we traversed the *A* phase. At last we had something quantitative to deal with!

The experiment was performed at various magnetic fields corresponding to various different Larmor frequencies. At the suggestion of our Cornell colleague, Robert Silsbee, the results were plotted as the difference between squares of liquid and solid frequencies respectively vs. the increment in pressure above the pressure corresponding to point *A*. To our delight, all the points fell on a universal curve, shown in Figure 7 corresponding to the equation $\omega^2 - \omega_0^2 = \Omega_A^2(T)$, where T was obtained from the extrapolated melting pressure. In this relationship, ω is the observed satellite line frequency and ω_0 is the solid frequency corresponding to the Larmor frequency of ^3He . The right-hand side corresponded to an increasing function of $1 - T/T_A$. This was interpreted as the development of an order parameter as the temperature de-

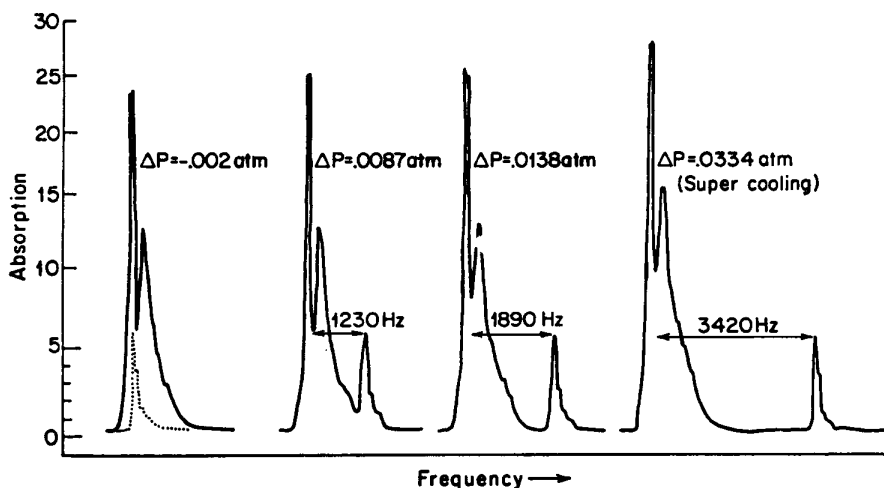


Figure 6. A sequence of NMR profiles taken in the cell of Figure 4 after the gradient was removed. The liquid signal in the *A* phase shifts away from the solid signal (corresponding to the Larmor frequency) as the sample is cooled. The shifted line abruptly disappears at point *B*.

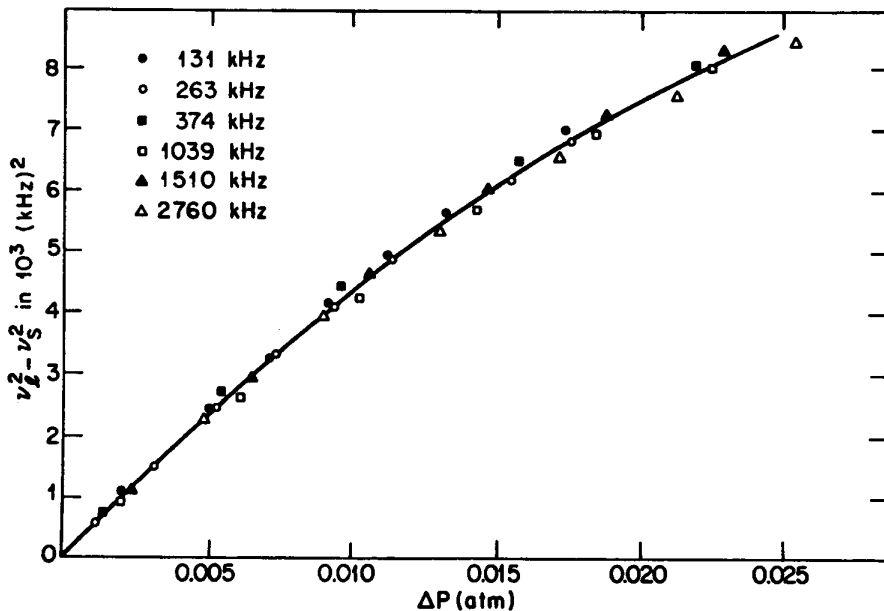


Figure 7. The differences between the squares of the liquid frequency and those of the solid (Larmor) frequency are plotted against the Pomeranchuk cell pressure as referred to the pressure at the A transition. The different symbols correspond to data taken at different magnet fields as indicated by the Larmor frequency associated with each symbol. All the data points fall on a *universal* curve.

creased. The Pythagorean relationship suggested that two magnetic fields were present in the problem, the external applied magnetic field and an internal field associated with an order parameter perpendicular to the applied magnetic field. As the temperature was lowered, the magnitude of the internal field varied from zero to approximately 30 gauss, which is much greater than the dipolar interaction field between two ^3He atoms separated by the mean distance between atoms in the liquid. A vector diagram demonstrating how the applied field and a perpendicular internal field combine to give the Pythagorean frequency shift formula is given in Figure 8.

By the early summer of 1972, it was completely clear to us that the strange phenomena seen during the previous six months could be clearly identified with liquid ^3He . We were therefore very anxious to correct the preliminary but erroneous interpretation given in our first publication. A second manuscript was prepared which described the results of our nuclear magnetic resonance experiments and which carefully argued that new phases of liquid ^3He had been discovered. This manuscript was submitted to *Physical Review Letters*, but unfortunately it was turned down by the referee. We were shocked by this development and spent a great deal of time trying to get the decision overturned. Ultimately, reason prevailed and the manuscript finally appeared.⁵⁰

At the time there was still no theoretical understanding of the strange drop in susceptibility at the B transition nor of the even stranger frequency shift in the A phase. Could the low susceptibility of the B phase be associated with singlet pairing? As mentioned earlier, s wave pairing was excluded for ^3He ,

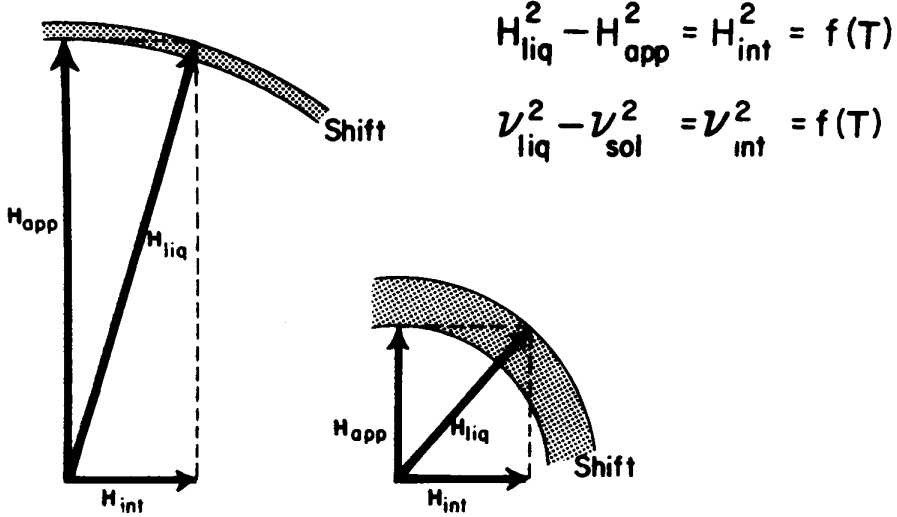


Figure 8. The effect of the internal field on the magnetic resonance frequency in $^3\text{He A}$. For a given temperature, the width of the shaded region corresponds to the size of the frequency shift away from the Larmor frequency. Diagrams for a large applied field and for a small applied field are shown.

but d wave pairing was possible and had been discussed by Emery and Sessler.²⁹ As for explaining the frequency shift, there were only vague suggestions that $^3\text{He A}$ was exhibiting a new type of antiferromagnetic behavior. Of course we discussed these issues with members of our theory group. Neil Ashcroft suggested that we should consider the possibility of p wave pairing and Vinay Ambegaokar pointed out the paper by Balian and Werthamer³¹ which actually treated p wave pairing. As it turned out, both of these suggestions were directly applicable to the B phase of liquid ^3He , at least.

A special p wave ($S = 1$) pairing state was hypothesized by Balian and Werthamer as mentioned in the introduction. This state corresponded to an order parameter with three spin components, $S_z = +1$, $S_z = 0$ and $S_z = -1$ i.e. $\uparrow\uparrow$, $1/\sqrt{2}(\uparrow\downarrow + \downarrow\uparrow)$ and $\downarrow\downarrow$ states. Since the $S_z = 0$ substate is "spinless", it does not contribute to the susceptibility. Thus the Balian Werthamer susceptibility should approach $2/3$ that of the normal Fermi liquid as $T \rightarrow 0$. In fact the B phase susceptibility is even smaller as a result of Fermi liquid interactions. Another property of the B phase which fits in with the Balian Werthamer state is the suppression of this phase by a magnetic field which was observed in some of our early Pomeranchuk cooling experiments. By about 0.6 tesla, the B phase no longer existed. As the field increased, the B phase was pushed to lower temperatures in favor of the A phase. The interpretation is that the higher magnetic field tends to suppress the spin zero ($\uparrow\downarrow + \downarrow\uparrow$) pairs. The $\downarrow\downarrow$ and $\uparrow\uparrow$ pairs can easily respond to the field merely by reorienting themselves.

The puzzle of the A phase frequency shift still needed to be solved. Within an amazingly short time, Anthony Leggett^{51,52} came forth with a brilliant solution to the problem. It was known that in conventional high temperature NMR experiments the main effect of the weak dipole-dipole interactions was

to broaden the NMR line. How could these weak dipolar interactions all conspire to provide a frequency shift corresponding to an internal field of 30 gauss at the lowest temperature attained in $^3\text{He A}$? Leggett introduced the hypothesis of spontaneously broken spin orbit symmetry (SBSOS) and, with the aid of sum rules, was able to obtain the proper order of magnitude for the frequency shift.⁵³ Let us consider how SBSOS can be responsible for a large frequency shift in the context of a superfluid with $l = 1$ pairing. The weak interaction between the tiny nuclear dipole moments is much less than one microkelvin, but somehow, in spite of much larger thermal fluctuations, the presence of Cooper pairs must lead to a coherent addition of all the dipole moments, giving rise to an effective internal field large enough to produce the observed frequency shifts. This comes about because all the Cooper pairs must be correlated, i.e. locked together so all of the nuclear moments must act together to provide the requisite effective internal magnetic field. By this means, we self-consistently generate a macroscopic dipolar interaction.

Let us consider two possible configurations for rotation of two nuclear dipoles about one another. One involves rotations such that the pair orbital angular momentum is parallel to the nuclear dipole moments and the other involves rotations where the pair orbital angular momentum is perpendicular to the dipole moments. Classically, this latter configuration has a lower energy and it turns out to be the favored state. Because of SBSOS, it will be highly favored, in fact. If we introduce an \vec{l} vector corresponding to the pair orbital angular momentum and define a vector \vec{d} corresponding to the direction of zero spin projection, then it would be energetically favorable for \vec{d} and \vec{l} to be parallel.

As a result of a set of fundamental equations of motion derived by Leggett⁵⁴ and discussed in the next section, we have the following picture for NMR in $^3\text{He A}$: A nuclear magnetic resonance experiment corresponds to an oscillation in the direction of \vec{d} about \vec{l} where the direction of \vec{l} is stabilized by the quasiparticles and the container boundaries. An important point here is that \vec{d} and \vec{l} are macroscopic vectors, with the restoring torque for oscillations of \vec{d} with respect to \vec{l} being provided by the macroscopic dipole interaction. This extra restoring torque is what gives rise to the frequency shift observed in $^3\text{He A}$.

The magnetic susceptibility of the *A* phase remains constant at the normal Fermi liquid value throughout the temperature range where it occurs. The explanation is as follows: In contrast to $^3\text{He B}$, the *A* phase belongs to a class of states known as equal spin pairing states containing only $\uparrow\uparrow$ and $\downarrow\downarrow$ pairs which can respond directly to any field change in a fashion similar to that of the normal Fermi liquid. The *p* wave pairing state put forward by Anderson and Morel³⁰ in 1961 is one possible member of this class. It is now believed that the early Anderson Morel state corresponds to the *A* phase of superfluid ^3He .

THE POST DISCOVERY PERIOD

The discovery experiments^{55,56} and Leggett's explanation of the *A* phase frequency shift⁵¹ were presented in the summer of 1972 at the 13th International Conference on Low Temperature Physics held in Boulder, Colorado. The discussions aroused great enthusiasm for further investigations, both experimental and theoretical. The first anomalous flow properties associated with possible superfluidity in the new phases were seen in a vibrating wire experiment conducted in a Pomeranchuk cell by a group at the Helsinki University of Technology.⁵⁷ Actual superfluid behavior was later demonstrated in fourth sound experiments by Yanof and Reppy⁵⁸ and Kojima, Paulson and Wheatley.⁵⁹ Ultrasound experiments, performed at Cornell (also in a Pomeranchuk cell) showed a pronounced attenuation peak near the *A* transition.⁶⁰ The peak was associated with the breaking of Cooper pairs near T_c as well as with the collective modes (pair vibrations of the order parameter). Experiments below the melting pressure were performed at La Jolla by adiabatically demagnetizing a powdered cerium magnesium nitrate paramagnetic salt contained directly in the liquid ^3He sample. The small grain powder made it possible to overcome the large thermal boundary resistance between the ^3He and the salt by providing a large area of contact. Measurements of the specific heat at the transitions into the new phases of ^3He gave curves characteristic of a BCS type transition with behavior below the transition showing a rapid rise with temperature, associated with pair breaking and the greater availability of quasiparticles, followed by a sharp drop at the transition.⁶¹ Above the transition, the typical linear temperature dependence of a normal Fermi liquid was found. These results are portrayed in Figure 9.

I have so far not mentioned the existence of a third phase, which could only exist in the presence of an applied magnetic field. Evidence for this was found in the discovery experiment where, in the presence of a magnetic field, instead of a single point corresponding to a change of slope in the pressure vs. time plot, there were two closely spaced points, each involving a change in slope in the melting pressure vs. time signature.⁶² Thus the *A* transition splits into two transitions in a magnetic field. Before hearing of these results, Vinay Ambegaokar and David Mermin had actually predicted theoretically that the *A* phase *should* split linearly in a magnetic field.⁶³ They showed that this was required by $l = 1$ BCS pairing and named the newly discovered phase A_1 . Particularly dramatic signatures of the splitting of the *A* transition into two transitions can be seen in the ultrasound data of Lawson *et al.*⁶⁴ (see Figure 10). The temperature width of the A_1 phase grows linearly with field at the rate of 60 μK per tesla all the way up to 10 tesla and beyond. The A_1 phase is believed to have only a single spin component, $|\uparrow\uparrow\rangle$.

Finally, the La Jolla group also investigated the phase diagram in a magnetic field⁶⁵ at pressures below melting pressure by studying the static magnetization of the liquid via superconducting quantum interference (SQUID) interferometry. The ^3He sample and the magnet supplying the applied magnetic field were contained in a separate tower surrounded by a superconduc-

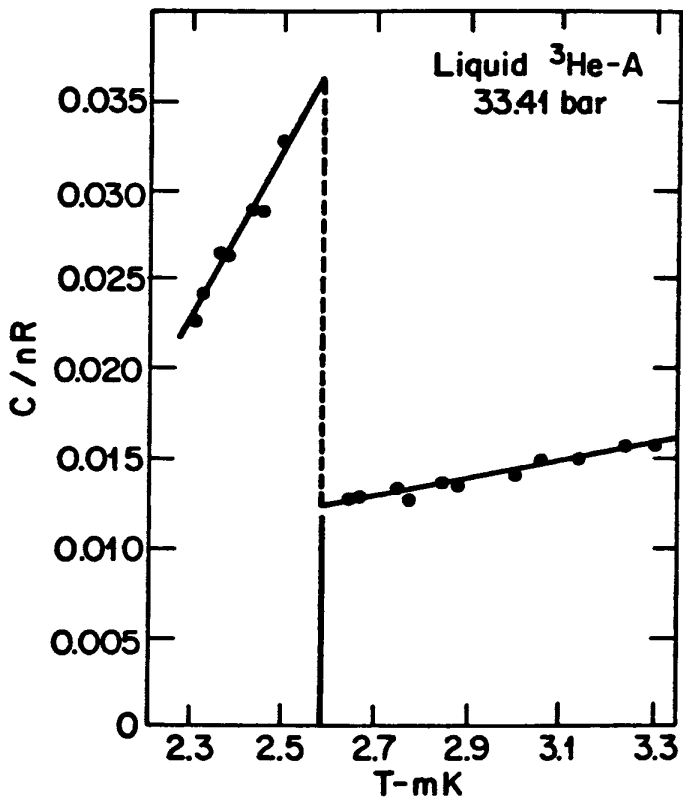


Figure 9. Early specific heat measurements of liquid ^3He near the superfluid transition.⁶¹ The shape is characteristic of a BCS pairing transition.

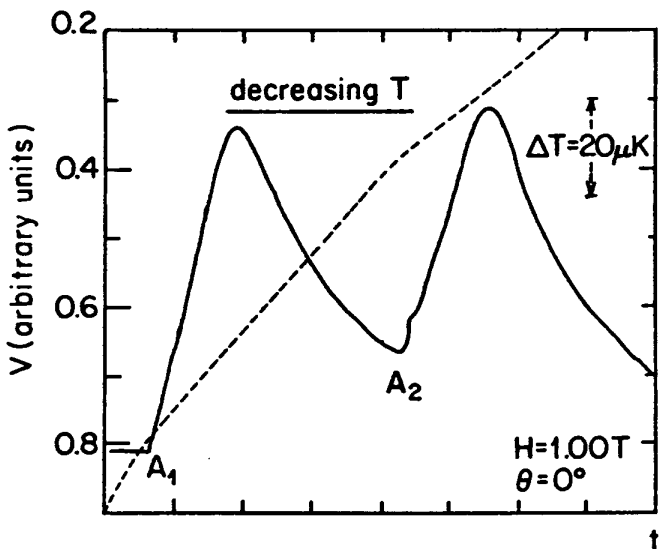


Figure 10. Sound attenuation data from a Pomeranchuk cooling run plotted against time in a 1 tesla magnetic field clearly showing the splitting of the A transition. A_1 and A_2 mark the two resulting transitions.⁶⁴ The attenuation peaks are associated with collective mode absorption and pair breaking near the transitions. The dashed line representing the melting pressure shows two kinks corresponding to the splitting of the A transition into the A_1 and A_2 transitions.

ting niobium magnetic shield. The liquid ^3He sample in the tower was maintained in good thermal contact with the cerium magnesium nitrate refrigerant in the main cell via a column of liquid ^3He . The most dramatic finding was the narrowing and finally the vanishing of the *A* phase in zero field at a point called the polycritical point as shown in Figure 11. All of the features discussed above are summarized by the schematic P-T-H phase diagram shown in Figure 12.

Soon after the discovery of the *A* and *B* phases at Cornell, low temperature laboratories all over the world began a broad effort to explore their properties. Condensed matter theorists became very actively involved in explaining the observed effects and predicting new phenomena. One of the main tasks to be undertaken was the proper identification of the respective order parameters corresponding to ^3He *A* and ^3He *B*. In our experimental group, we

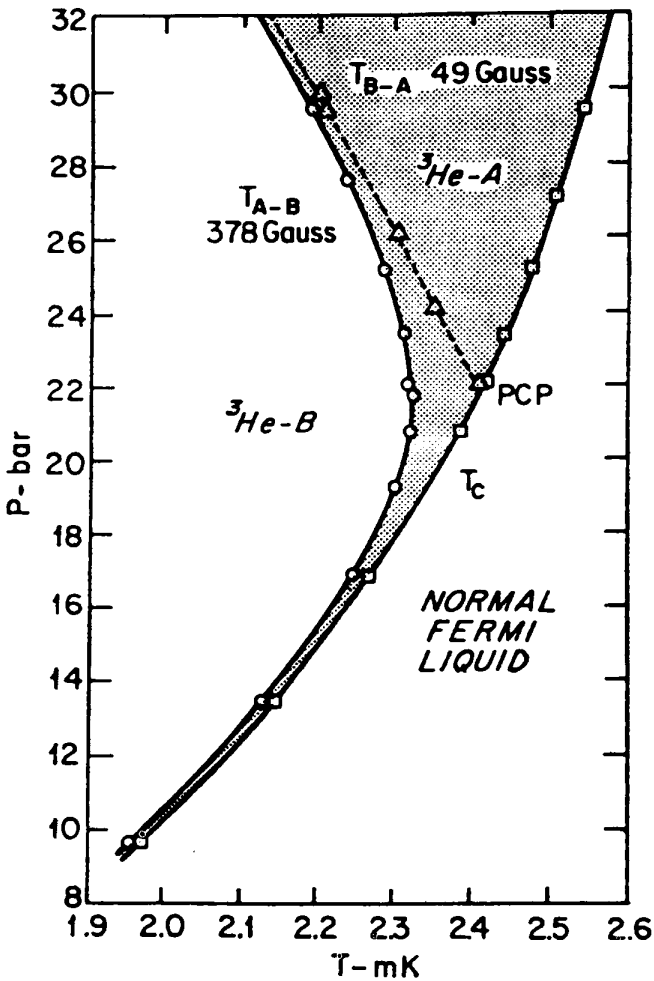


Figure 11. Experimental data of Paulson, Kojima and Wheatley.⁶⁵ At the lowest magnetic field, the *A* phase is not present below the polycritical point PCP at about 22 bar. In a larger magnetic field, the *B* phase is suppressed in favor of the *A* phase even at the lowest pressure and the polycritical point disappears.

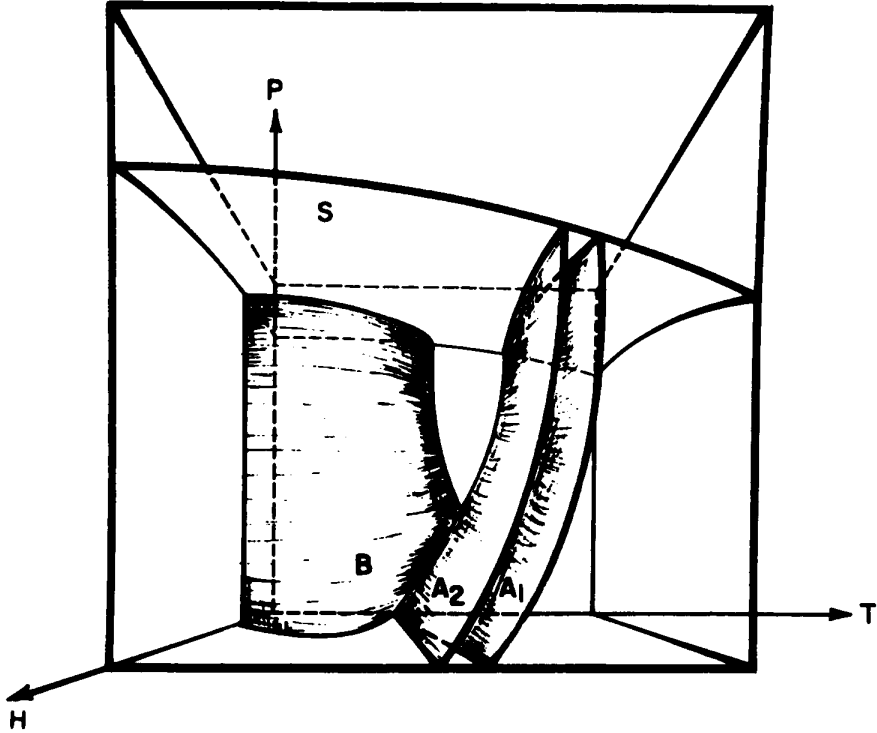


Figure 12. A schematic P-T-H diagram showing the general topology of the phase diagram of the superfluid phases, A, A₁ and B of liquid ³He. The A₁ phase occurs between the surfaces labeled A₁ and A₂. The A phase occurs at temperatures below the boundary labeled A₂. The boundary between phases A and B is labelled B. The surface labelled S corresponds to the melting curve.

adopted the working hypothesis that ³He A corresponded to the p wave equal spin pairing state first considered by Anderson and Morel³⁰ in 1961 and that ³He B corresponded to the state suggested by Balian and Werthamer³² in 1963. As mentioned in the previous section, these states were at least consistent with the Cornell discovery experiments.

Both the Anderson Morel and the Balian Werthamer states of p wave pairing are states with total $L = 1$ and total $S = 1$. The Anderson Morel state is an orbital $m = 1$ state along some direction \hat{l} and a spin $m = 0$ state along some direction \hat{d} . Recall that we introduced \hat{d} as the direction of zero spin projection earlier in our discussion. We express the Anderson Morel order parameter as the product between an orbital part in configuration or momentum space and a part in spin space, i.e.,

$$\psi_{AM} = (\text{orbital part}) \times (\text{spin part}).$$

If we consider only angular dependence, the Anderson Morel order parameter is defined as

$$\psi_{AM} \sim e^{i\varphi} \sin \theta \left[\frac{1}{\sqrt{2}} (\downarrow\uparrow + \uparrow\downarrow) \right],$$

where the spherical harmonic $Y_{11} \sim e^{i\varphi} \sin \theta$ defines a polar axis \hat{l} corresponding to the direction of the pair orbital angular momentum. In the above expression for the spin triplet pair wave function the spin part appears along the \hat{d} axis, so that only the $(\downarrow\uparrow + \uparrow\downarrow)$ component occurs. For the case of the Anderson Morel state, we see that the spin part of the order parameter does *not* depend on any orbital variables but is a *constant* in orbital space; i.e., in k space, every point on the Fermi surface has the same \hat{d} . We discussed earlier how a classical argument involving the dipolar interaction combined with spontaneously broken spin orbit symmetry would favor the state for which $\hat{l} \parallel \hat{d}$. Taking this into account we sketch the AM order parameter in k space in Figure 13a. The small arrows correspond to the \hat{d} vector and the large arrow corresponds to \hat{l} . One of the striking features of this order parameter is the orbital anisotropy, with nodes at $\theta = 0$ and $\theta = \pi$. The behavior of the BCS energy gap follows that of the order parameter so that gap nodes also appear at $\theta = 0$ and π as shown in Figure 13b. The full three dimensional picture is obtained by a revolution about the \hat{l} axis. The patterns in the orientation of \hat{l} as a function of position in the liquid are highly analogous to patterns found in liquid crystals. These patterns have been named textures. Ambegaokar, de Gennes and Rainer⁶⁶ have shown that the \hat{l} vector will be *perpendicular* to the walls of the containers. This boundary condition plays an important role in determining the texture pattern in liquid ^3He A. The direction of \hat{l} is also sensitive to flow and to the applied magnetic field.

The spin state $\frac{1}{\sqrt{2}}(\uparrow\downarrow + \downarrow\uparrow)$ can be rotated in spin space to give the equal spin pairing version of the Anderson Morel order parameter,

$$\psi_{AM} \sim e^{i\varphi} \sin \theta [(|\uparrow\uparrow\rangle + e^{i\Phi} |\downarrow\downarrow\rangle)],$$

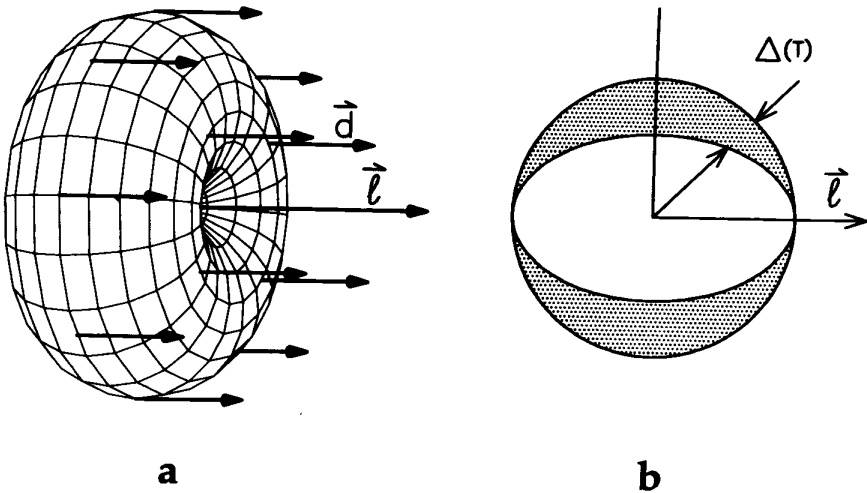


Figure 13. (a) A three dimensional representation of the Anderson-Morel order parameter. The vector \hat{l} at the center defines the axis of the order parameter. Along this axis, the amplitude is zero corresponding to $\sin \theta$ dependence where θ is the polar angle with respect to \hat{l} . The vector \hat{d} has the *same* direction for all points on the Fermi surface.

(b) The anisotropic energy gap is indicated by the shaded region. The two nodes along \hat{l} are clearly shown.

where Φ is a phase factor, which is helpful in discussing longitudinal NMR experiments. This representation shows that the Anderson Morel order parameter can be characterized by a spin configuration with only $|\uparrow\uparrow\rangle$ and $|\downarrow\downarrow\rangle$ states, as mentioned in our earlier discussions. The A_1 phase has the orbital properties including the gap nodes described by the Anderson Morel state but has only $|\uparrow\uparrow\rangle$ spin pairs.

We shall now discuss the Balian Werthamer state. The simplest possible Balian Werthamer state is the 3P_0 state, represented by the wave function

$$\psi_{BW} \sim Y_{1,-1} |\uparrow\uparrow\rangle + Y_{10} |\uparrow\downarrow + \downarrow\uparrow\rangle + Y_{11} |\downarrow\downarrow\rangle$$

so that all three spin species are included. Hence we do not have an equal spin pairing state. Since the 3P_0 state has total $J=0$, it will be a spherically symmetric state. When this is taken into account, it is customary to specify this simple Balian Werthamer state in terms of the vector \hat{d} by $\hat{d}(k) = \text{constant} \times \hat{k}$ which has the necessary spherical symmetry. Notice that in contrast to the Anderson Morel state, \hat{d} depends on \hat{k} .

The simple state discussed above does not perfectly represent the order parameter of superfluid $^3\text{He B}$. As far as the most important interactions are concerned, the energy will not change when the spin and orbital coordinates are rotated with respect to one another. Thus we could rotate \hat{d} about some axis \hat{n} to get $\hat{d} = R\hat{k}$, where R is an arbitrary rotation about an arbitrary axis \hat{n} for superfluid $^3\text{He B}$. This degeneracy is broken when the small dipolar interaction is taken into account, which results in a rotation of the spin coordinates relative to the orbital coordinates by an angle of 104° as discussed below. This subtle anisotropy allows textures associated with liquid crystal like behavior to be observed in superfluid $^3\text{He B}$. Nevertheless the overall orbital symmetry of the order parameter is still spherical, leading to an isotropic energy gap similar to that of s wave superconductors. Figure 14a shows the order parameter with \hat{d} twisted about some axis \hat{n} by 104° , and Figure 14b shows the isotropic energy gap.

I have now outlined the basic properties of the Anderson Morel and the Balian Werthamer states which were provisionally identified with $^3\text{He A}$ and $^3\text{He B}$, respectively. An important question still remained to be addressed. The early studies of the possible order parameters of p wave pairing showed that the Balian Werthamer state would have a lower free energy and therefore should always be the preferred state. On the other hand the existence of an Anderson Morel type state in ^3He was firmly established by the experiments. The apparent discrepancy was resolved by Anderson and Brinkman⁶⁷ who introduced the idea of spin fluctuation feedback which led to a mechanism for a stable Anderson Morel phase. (Recall our previous discussion of the possible role of spin fluctuations by Layzer and Fay.) Since the pairing mechanism is intrinsic, thus involving the ^3He quasiparticles themselves, any modification in the status of the helium quasiparticles should affect the pairing mechanism, including the onset of pairing itself. Anderson and Brinkman showed that this feedback effect could indeed lead to a stable Anderson

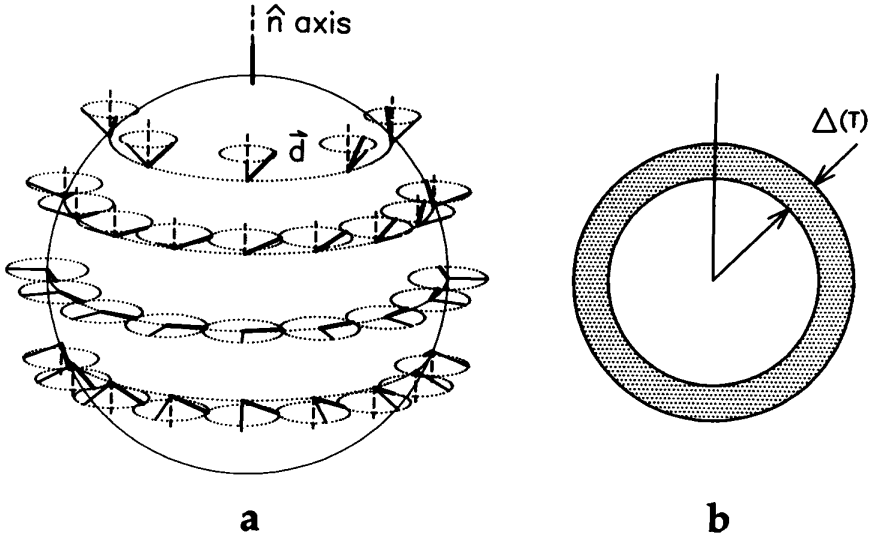


Figure 14. (a) The order parameter for superfluid $^3\text{He B}$ showing \vec{d} vectors (represented by thick lines) rotated by 104° about a vector \hat{n} from the radial directions (thin lines) for all points on the Fermi sphere. The rotation axis \hat{n} points in the vertical direction.

(b) The isotropic energy gap of the Balian Werthamer order parameter is indicated by the shaded region. Ordinary s -wave superconductors also have isotropic energy gaps.

Morel phase in zero magnetic field, which was renamed the Anderson Brinkman Morel phase or ABM state. These studies led to the general acceptance that the Anderson Brinkman Morel state corresponded to $^3\text{He A}$ and the Balian Werthamer state corresponded to $^3\text{He B}$. More recent comprehensive studies of a variety of pairing mechanisms conducted by Rainer and Serene have not changed this conclusion.⁶⁸

No general discussion of superfluid ^3He would be complete without a treatment of the macroscopic nuclear dipole interaction and its role in the dramatic NMR effects observed experimentally. The general scheme for calculating the dipolar interaction is to take a quantum mechanical average of the dipolar Hamiltonian over the pair wave function (order parameter). It can then be shown that the dipolar free energies are given by

$$\Delta F_D = \begin{cases} -\frac{3}{5}g_D(T)[1 - (\vec{d} \cdot \vec{\ell})^2], & \text{A phase} \\ \frac{4}{5}g_D(T)\{\cos \theta + 2 \cos^2 \theta + \frac{3}{4}\}, & \text{B phase} \end{cases}$$

where

$$g_D \approx 10^{-3} \left(1 - \frac{T}{T_c} \right) \text{ ergs/cm}^3.$$

Therefore, to minimize the free energy, \vec{l} and \vec{d} must be parallel for the case of the ABM state (A phase) in agreement with our earlier qualitative discussion. For the BW state, a simple calculation shows that the dipole energy is minimized for $\theta = \cos^{-1}(-\frac{1}{4}) = 104^\circ$ justifying our earlier statement.

Making use of the macroscopic dipolar interaction, Leggett⁵² derived a set

of coupled equations giving a complete description of the spin dynamics of superfluid ^3He . His equations of motion are

$$\begin{aligned}\dot{\vec{S}} &= \gamma \vec{S} \times \vec{H} + R_D(T) \\ \dot{\vec{d}} &= \vec{d} \times \gamma \vec{H}_{\text{eff.}} = \vec{d} \times \gamma \left(\vec{H} - \frac{\gamma \vec{S}}{\chi} \right)\end{aligned}$$

The first term in the first Leggett equation corresponds to Larmor precession (ordinary NMR) whereas the second term is a restoring torque resulting from the dipolar interaction. The second equation describes the precession of \hat{k} in an effective field. The motion of \vec{d} and that of \vec{S} are coupled. In the A phase $R_D(T)$ takes on a particularly simple form:

$$R_D(T) = \frac{6}{5} g_D(T) (\vec{d} \times \vec{\ell}) (\vec{d} \cdot \vec{\ell})$$

It is this term which gives rise to the frequency shift found in superfluid ^3He A. The coupled motions of \vec{S} and \vec{d} for ^3He A as predicted by the Leggett equations are illustrated in Figure 15, which shows the free precession following a 10° tipping pulse. The spin vector precesses about the applied steady mag-

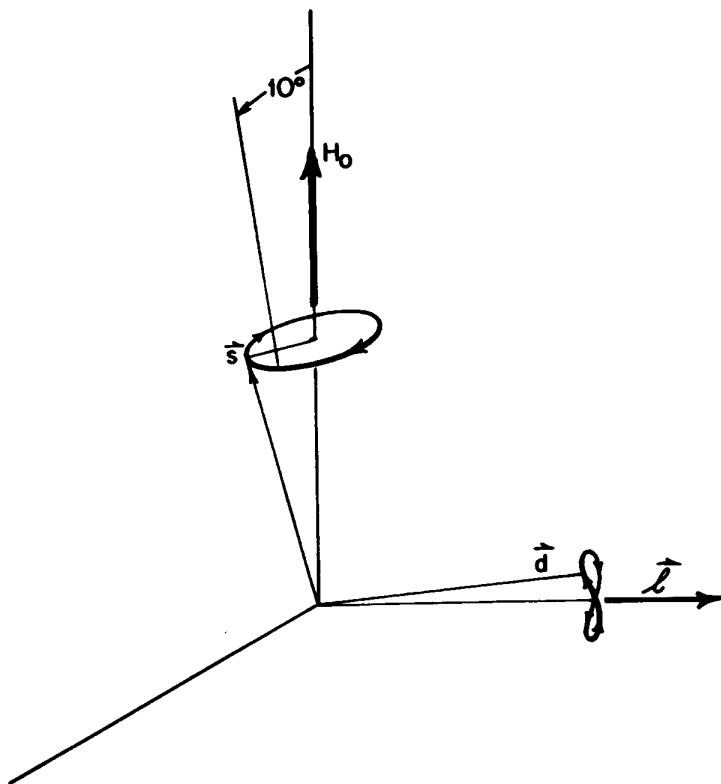


Figure 15. The free precession of the spin vector and the \vec{d} vector after a small tipping pulse according to the Leggett equations.

netic field describes an ellipse, while the corresponding motion of the unit vector d describes a figure eight on the unit sphere.⁶⁹

With this beautiful theory of the dynamics of the order parameter, Leggett calculated the frequency shift for the transverse (ordinary) NMR for both the ABM and the Balian Werthamer (BW) states. The calculation of the frequency shift for the ABM state gave the Pythagorean relationship $\omega^2 - \omega_0^2 = \Omega_A^2(T)$ found in the discovery experiments. The BW state showed no transverse frequency shift, again in agreement with experiment. The Leggett equations of motion also predicted the existence of longitudinal resonance in both the ABM and BW states. Longitudinal resonance experiments are performed by orienting the radiofrequency coil parallel to the applied steady magnetic field H_0 so that $H_{rf} \parallel H_0$. For the case of ordinary (transverse) NMR, $H_{rf} \perp H_0$. At the time of the discovery experiment we speculated on this possibility for the A phase based on the Pythagorean relationship which implied an internal field perpendicular to the applied field (see Figure 8). We had no idea that the B phase would also manifest a longitudinal magnetic resonance. Longitudinal resonance signals were observed by Osheroff and Brinkman⁷⁰ at the Bell Telephone Laboratories in both the A and B phases. Later we observed longitudinal magnetic resonance in the A phase at Cornell.⁷¹ (Typical longitudinal resonance frequencies ranged up to about 100 kHz in ^3He A at melting pressure.) The longitudinal frequency in ^3He A, $\Omega_A(T)$, is related to the longitudinal frequency in ^3He B, $\Omega_B(T)$ by the ratio

$$\left[\frac{\Omega_B(T)}{\Omega_A(T)} \right]^2 = \frac{5}{2} \frac{\chi_B}{\chi_A}.$$

Longitudinal signals were also observed by Webb *et al.*⁷² by applying a step in the steady field and observing radiofrequency longitudinal ringing with SQUID detectors.

An important feature which sets superfluid ^3He apart from the more conventional superconductors and superfluid ^4He is the presence of internal degrees of freedom of the order parameter. So far, we have discussed mainly the spin degrees of freedom and how they relate to the NMR experiments. Observations have also revealed a variety of interesting phenomena related to the orbital degrees of freedom. For example, the orbital anisotropy of the A phase leads to anisotropic flow properties. Mermin and Ho⁷³ showed that this completely altered the character of quantized circulation, leading to novel mechanisms for the decay of supercurrents. The anisotropy of the superfluid density was first discovered by Berthold, Giannetta, Smith and Reppy⁷⁴ at Cornell using torsional oscillator techniques. Figure 16 shows their results for two orientations of the A phase obtained by appropriately orienting the external magnetic field.

One area in which we have been particularly actively involved is the study of sound propagation in superfluid ^3He . As we mentioned earlier, the sound attenuation mechanisms in the superfluid are mainly associated with pair breaking when $\hbar\omega_{\text{sound}} \geq 2\Delta$ and with collective modes corresponding to in-

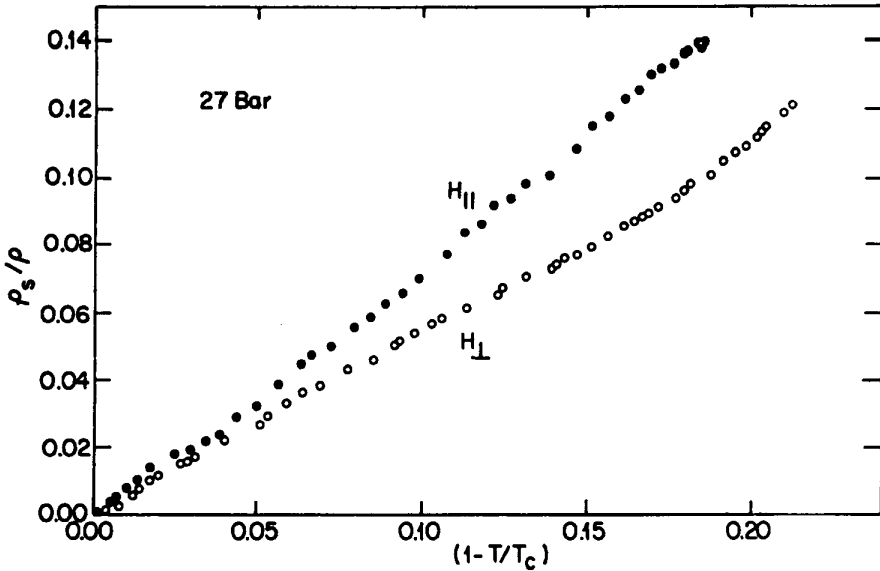


Figure 16. Anisotropy of the superfluid density as determined in torsional oscillator measurements by Berthold, Giannetta, Smith and Reppy.⁷⁴ Two different orientations of the order parameter are shown, where the orientation is controlled by the applied magnetic field via the dipolar interaction.

ternal vibrations of Cooper pairs. Because they are governed by a macroscopic order parameter, the Cooper pairs are coherently excited and thus vibrate in phase. The pair vibration modes which couple to density fluctuations can be excited by sound waves. The collective modes are analogous to excited states of atoms, but for the case of superfluid ^3He , the whole liquid sample participates in the collective motion, providing a spectacular example of London's quantum mechanics on a macroscopic scale, this time being associated with the orbital internal degrees of freedom.

The energy gap of $^3\text{He A}$ has two point nodes where the \hat{l} axis intersects the Fermi surface. Thus pair breaking can take place via these nodes all the way to absolute zero. The pair vibration modes exhibit anisotropy in superfluid $^3\text{He A}$. In fact, the first evidence for orbital anisotropy in $^3\text{He A}$ was seen in early ultrasound experiments by Lawson *et al.*⁷⁵ and Roach *et al.*⁷⁶ The B phase, on the other hand, has an isotropic energy gap and so the breaking of pairs takes place only above a finite threshold called the pair breaking edge. It is thus possible to study the collective modes of $^3\text{He B}$ without the complications of pair breaking as long as the energy of a sound quantum $\hbar\omega$ is less than 2Δ . At the lowest temperatures a vanishing number of excited quasiparticles is present so any quasiparticle collision broadening of the collective modes is almost completely negligible. Thus very narrow sound absorption lines associated with collective modes in superfluid $^3\text{He B}$ are expected. Therefore the analogy between pair vibrations and the excited states of atoms is best illustrated by the collective modes in superfluid $^3\text{He B}$.

Our more recent ultrasound experiments utilized nuclear adiabatic demagnetization methods to cool the liquid ^3He down into the superfluid phase. Modern experiments on superfluid ^3He employ this cooling tech-

nique. The technique had been pioneered by Nicholas Kurti and his co-workers at Oxford University⁷⁷ but was first used to cool liquid ^3He by John Goodkind and his students at the University of California at San Diego.⁷⁸ Nuclear adiabatic demagnetization of a bundle of copper wires or plates to cool liquid ^3He well into the superfluid regime was developed into a standard technology by Olli Lounasmaa and his group at Helsinki University of Technology.⁷⁹ The technique had the advantage of making accessible pressures below melting pressure for the liquid ^3He sample just as in the case of adiabatic demagnetization of paramagnetic salts, but much lower temperatures (well below 1 mK) also became available. To overcome the large thermal boundary resistance between the ^3He sample and the copper bundle, a sintered silver heat exchanger with very high surface area was placed inside the ^3He cell and firmly anchored thermally to the wall of the cell.

The two collective modes we studied in superfluid B are called the imaginary squashing mode and the real squashing mode. They correspond to two different types of periodic distortions of the energy gap. These modes were first studied theoretically by Wölfle,⁸⁰ Serene,⁸¹ and Maki.⁸² Both of these modes are in the total angular momentum state $J = 2$ in contrast to the $J = 0$ ground state associated with the B phase order parameter. We are neglecting the effect of the 104° rotation of the spin coordinates of the ground state relative to the orbital coordinates which is not important for our ultrasound studies. The real squashing mode couples much more weakly to sound than the imaginary squashing mode. These modes are excited by ultrasound at frequencies given by the following expressions:

$$\hbar\omega_{\text{sound}} = \begin{cases} \sqrt{\frac{12}{5}}\Delta(T), & \text{Imaginary Squashing Mode} \\ \sqrt{\frac{8}{5}}\Delta(T), & \text{Real Squashing Mode} \end{cases}$$

Fixed frequency quartz piezoelectric sound transducers driven at harmonic frequencies between 40 and 120 MHz were used in these experiments so that the profile of the sound absorption line had to be determined by sweeping $\Delta(T)$ via varying the temperature rather than by sweeping the frequency. Sound attenuation experiments were performed at Cornell by Giannetta *et al.*⁸³ A complete temperature sweep is shown in Figure 17 based on the Cornell data where the sound attenuation data is plotted against the temperature. Clearly displayed are three well-differentiated peaks. At the highest temperature is the broad peak associated with pair breaking. The intermediate peak is the imaginary squashing mode. The attenuation is so large for these two high temperature peaks that it could not be measured in our experiment. The small, very narrow low temperature peak is the real squashing mode. The small size of this peak is directly attributable to the weak coupling of the real squashing mode to sound. Observations of the real squashing mode were made by Mast *et al.*⁸⁴ at the same time as those of Giannetta *et al.*

The real squashing mode and the imaginary squashing mode display spectacular effects in the presence of applied magnetic fields. These effects were first revealed in the experiments of Avenel, Varoquaux and Ebisawa⁸⁵ for the

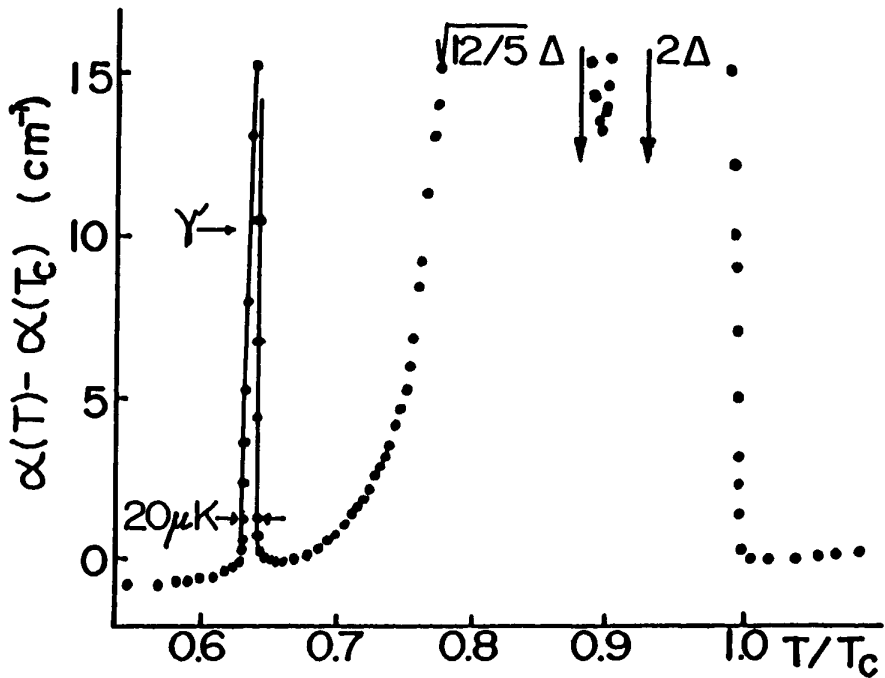


Figure 17. Attenuation of ultrasound in superfluid $^3\text{He B}$ showing the pair breaking peak, the imaginary squashing mode peak and the narrow real squashing mode peak.⁸³ The very strong attenuation associated with pair breaking and the imaginary squashing mode made it impossible to observe the peak maxima for these two peaks. The data were taken at a constant sound frequency during a temperature sweep.

real squashing mode, which exhibited a five-fold Zeeman splitting corresponding to a $J=2$ excited state, linear in field for low fields as shown in Figure 18. A similar five-fold splitting for the imaginary squashing mode has been observed at Cornell by Movshovich *et al.*⁸⁶ using special techniques. The splittings of the real squashing mode and the imaginary squashing mode were first predicted by Tewordt and Schopohl.⁸⁷ A spectrum schematically showing these modes is provided in Figure 19. The left side of the figure shows the spectrum of a bulk sample of superfluid $^3\text{He B}$ for zero applied magnetic field and the right side shows the five-fold splittings of the $J=2$ excited modes in a magnetic field. These spectra provide spectacular examples involving the roles of both magnetic and orbital degrees of freedom in the excited state pair wave functions. These phenomena are further dramatic manifestations of London's idea of quantum mechanics on a macroscopic scale, this time in excited modes involving spin and orbital degrees of freedom simultaneously.

SOME IMPORTANT DEVELOPMENTS

Superfluid ^3He is a complex and beautiful system where the internal degrees of freedom play a prominent role, leading to a large array of phenomena not seen in conventional s wave superconductivity or in superfluid ^4He . In con-

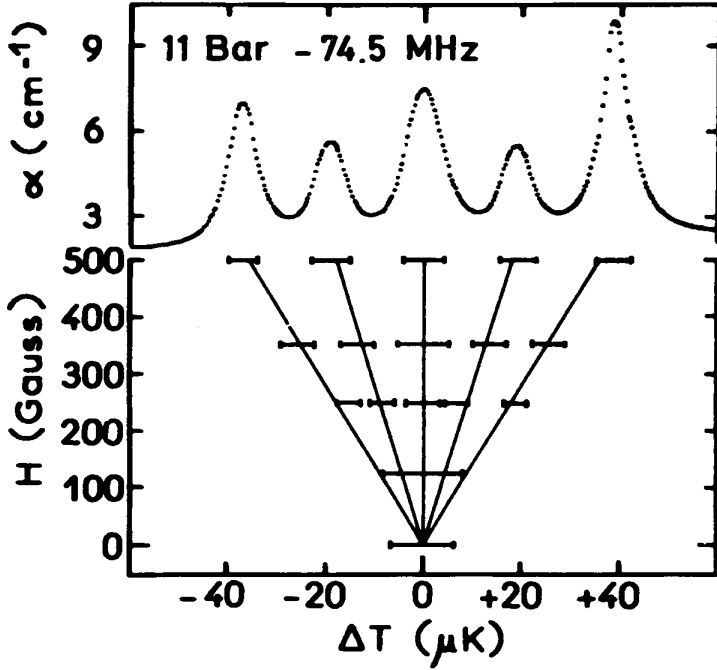


Figure 18. Splitting of the real squashing mode in a magnetic field as observed by Avenel, Varoquaux and Ebisawa.⁸⁵ Also shown are the attenuation peaks for the sound propagation direction perpendicular to the magnetic field.

trast to conventional superconductors, the pairing is intrinsic, not relying on the exchange of phonons via an ionic lattice. The complex phase diagram shows three different superfluid phases of liquid ^3He , each with its own unique set of properties. We have already discussed the way in which London's idea of quantum mechanics on a macroscopic scale applies to the nuclear magnetic resonance experiments and the studies of collective modes excited by sound. Interesting effects seen in other branches of condensed matter physics have also been observed in superfluid ^3He . We have only touched upon the anisotropic flow properties associated with the anisotropy of the energy gap and the gap nodes in the A and the A_1 phases. In addition, satellite NMR lines in ^3He A, first seen for longitudinal resonance by Avenel *et al.*⁸⁸ and for transverse resonance by Gould and Lee,⁸⁹ have been interpreted⁹⁰ as solitons resembling thin domain walls where the orientations of the \hat{l} and \hat{d} vectors abruptly change.

The phenomenon of second sound, seen previously in superfluid ^4He , has actually been observed in the A_1 phase of superfluid ^3He by Corruccini and Osheroff,⁹¹ where it involves a wave-like propagation of heat and simultaneously the propagation of a spin density wave. This is related to the fact that the superfluid density in the two fluid model contains only spin up pairs. Since spin down pairs are not present in the order parameter of the A_1 phase, the spin down quasiparticle density comprising the normal fluid density remains large at the lowest temperatures. This condition is not obeyed for the A and B phases where second sound is highly damped due to the relative

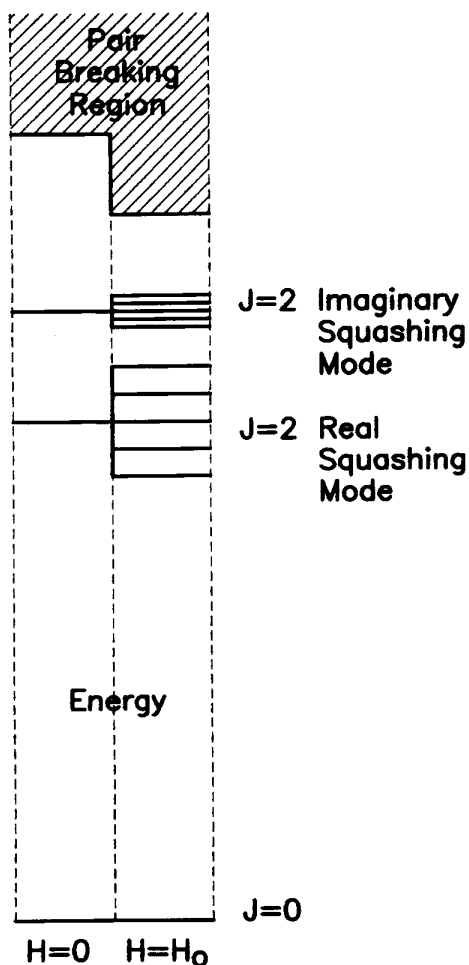


Figure 19. A schematic diagram showing the collective modes of superfluid $^3\text{He B}$ discussed in the text. The left hand side of the diagram shows the zero field spectrum. The five fold degenerate $j = 2$ real squashing and imaginary squashing modes are shown as well as the pair breaking edge which is crudely analogous to the ionization energy of an atom. The right hand side of the diagram shows the five fold Zeeman splitting of these collective modes. The g factor of the imaginary squashing mode is smaller than that of the real squashing mode. The pair breaking edge occurs at a lower energy in a magnetic field partially as a result of gap distortion by the field.

scarcity of normal fluid. According to the two fluid model, the heat is associated with the normal fluid density. A wave-like propagation of heat will involve a wave-like propagation of alternate regions of high normal fluid density and high superfluid density, leading to the propagation of a spin density wave.

In recent years, studies of superfluid ^3He have been conducted in rotating cryostats at Cornell, the Helsinki University of Technology, the University of California at Berkeley, and most recently the University of Manchester. The study of persistent currents in superfluid $^3\text{He A}$ and $^3\text{He B}$ by John Reppy and his coworkers at Cornell has furnished the final proof that both phases are indeed true superfluids.^{92,93} The very complexity of superfluid ^3He leads to a rich variety of vortex behavior which has been the main effort at

Helsinki in recent years. A vast experimental and theoretical effort has been under way to classify and understand this fascinating vortex behavior.^{94,95} Finally Richard Packard and his associates have studied vortices in ^3He B using the vibrating wire technique developed by Vinen⁹⁶ for superfluid ^4He and have shown directly the role of Cooper pairs in the vortices.⁹⁷ A major advance has also been made by physicists at the Kapitza Institute in Moscow. They have been able to stabilize a large region of superfluid ^3He with the spins uniformly precessing at a single frequency in spite of the presence of a significant magnetic field gradient. Spin supercurrents played a vital role in attaining these homogeneously precessing domains. One of the most important results to emerge from this work has been the observation of the Josephson effect involving spin currents.⁹⁸

Superfluid ^3He research may have some bearing on studies of exotic superconductivity.⁹⁹ In particular, complex (non-s wave) order parameters have been proposed for heavy fermion and high T_c superconductors. In the latter case some very recent tunneling¹⁰⁰ and magnetometer¹⁰¹ experiments provide compelling evidence that the high temperature superconducting cuprates can exhibit d wave pairing. Work at various laboratories around the world is under way to verify this result. With regard to the heavy fermion superconductors, UPt_3 has turned out to be a very promising candidate for $l > 0$ pairing.^{99,102} It has a complex superconducting phase diagram with several superconducting phases as well as thermal properties which are consistent with gap nodes.

The cooling techniques and thermometry techniques developed by laboratories around the world for studies of superfluid ^3He have already been useful. For example, the phase transitions of superfluid ^3He along the melting curve can serve as thermometric fixed points. The nuclear adiabatic demagnetization techniques have been used at the Helsinki University of Technology to study nuclear magnetic ordering of solids in the sub-microkelvin temperature range.¹⁰³

In the realm of astrophysics, theoretical studies of the neutron rich interior of neutron stars have indicated the possibility of a 3P_2 neutron superfluid ground state order parameter.¹⁰⁴ In addition, superfluid ^3He can serve as a model system for processes in the early universe. Gregory Volovik¹⁰⁵ has been particularly active in drawing analogies between the phases of liquid ^3He and phases of the vacuum in the early universe. As the universe cooled, it made transitions from a featureless hot universe to the universe we know today via phase transitions involving broken symmetry. Already some experimental work in superfluid ^3He has been performed to pursue this analogy.^{106,107,108}

CONCLUSION

Superfluid ^3He has provided an enormous amount of fun to the participants in the field. The role of internal degrees of freedom of the Cooper pairs has given new meaning to London's proposal that quantum mechanics on a macroscopic scale can describe superfluidity.

In addition, studies of this exotic superfluid have stimulated investigators in a wide variety of other fields. We have discussed ways in which superfluid ^3He research can be linked to high T_c superconductivity, heavy fermion superconductivity and liquid crystals in condensed matter physics. Examples of soliton behavior have also been observed in superfluid ^3He . The NMR technique employed in our experiments involved one of the very earliest applications of magnetic resonance imaging, now a widely accepted diagnostic technique in medicine and biology.

Phenomena in superfluid ^3He can also be related to astrophysics. The states of p wave pairing in superfluid ^3He may have their analogies to possible pairing states in neutron stars. The superfluid phase transitions in ^3He may also serve as a model for transitions which occurred in the early universe.

One may take the point of view that the importance of a field of research is related to its impact on other areas of science. In spite of the fact that superfluid ^3He exists in a difficult temperature range attainable only by highly specialized techniques, both the techniques and the results of superfluid ^3He investigations have indeed had important influences on diverse fields of research.

We gratefully acknowledge the National Science Foundation for providing support to our research program for more than 36 years. We have also benefited from support by the Advanced Research Projects Agency for a shorter time, during an important period spanning some of the most exciting developments discussed herein.

REFERENCES

1. Kamerlingh Onnes, H., Proc. Acad. Sci. Amsterdam **11**, 168 (1908).
2. Kamerlingh Onnes, H., Leiden Comm. **1226**, 124c (1911) Suppl. **35** (1913).
3. Simon, F., Nature, London **133**, 529 (1934).
4. Atkins, K. R., Liquid Helium, Cambridge University Press, Cambridge, 1959, p. 2.
5. Keesom, W. H. and K. Clusius, Proc. Royal Acad. Amsterdam **35**, 307 (1932). \ Keesom, W. H., and A. P. Keesom, Proc. Royal Acad. Amsterdam **35**, 736 (1932).
6. Daunt, J. G. and K. Mendelssohn, Proc. Royal Society A **170**, 423, 439 (1939).
7. Kapitza, P. L., Nature, London **141**, 74 (1938), and Kapitza, P. L., J. Phys. Moscow **4**, 181 (1941).
8. Allen, J. F. and H. Jones, Nature, London **141**, 75 (1938) and Proc. Camb. Phil. Soc. **34**, 299 (1938).
9. Landau, L. D., J. Phys., Moscow **5**, 71 (1941).
10. Tisza, L., J. Phys. Radium I, 165 and 350 (1940).
11. Andronikashvili, E. L., J. Phys. Moscow **10**, 201 (1946).
12. Peshkov, V., J. Phys. (USSR) **8**, 381 (1944).
13. London, Fritz, Superfluids, Vol. II, John Wiley and Sons, Inc., New York, (1954).
14. Ginzburg, V. L. and L. D. Landau, Zh. Eksperim i Teor. Fiz. **20**, 1064 (1950).
15. Maxwell, E., Phys. Rev. **78**, 477 (1950).
16. Reynolds, C. A., B. Serin, W. H. Wright and L. B. Nesbitt, Phys. Rev. **78**, 487 (1950).
17. Bardeen, J., L. N. Cooper and J. R. Schrieffer, Phys. Rev. **108**, 1175 (1957).
18. Cooper, L. N., Phys. Rev. **104**, 1189 (1956).
19. London, F. and H. London, Proc. Roy. Soc. (London) **A149**, 71 (1935).
20. London, F., Superfluids, Vol. I, John Wiley and Sons Inc., New York (1950).
21. Deaver, B. S. and W. M. Fairbank, Phys. Rev. Lett. **7**, 43 (1961).

22. Doll, R. and M. Näbauer, *Phys. Rev. Lett.* **7**, 51 (1961).
23. Josephson, B. D., *Phys. Lett.* **1**, 251 (1962).
24. Landau, L. D., *Zh. Eksp. i Teor. Fiz.* **30**, 1058 (1956); *Soviet Phys. JETP* **3**, 920 (1957), and Landau, L. D., *Zh. Eksp. i Teor. Fiz.* **32**, 59 (1957); *Soviet Phys. JETP* **5**, 101 (1957).
25. Wheatley, J. C. in *Progress in Low Temp. Physics*, Vol. VI, ed. C. J. Gorter, North-Holland Publishing, Amsterdam (1966), p. 183.
26. Keen, B. E., P. W. Mathews and J. Wilks, *Phys. Lett.* **5**, 5 (1963).
27. Abel, W. R., A. C. Anderson and J. C. Wheatley, *Phys. Rev. Lett.* **17**, 74 (1966).
28. Pitaevskii, L. P., *Zh. Eksp. i Teor. Fiz.* **37**, 1794 (1959); *Soviet Phys. JETP* **10**, 1267 (1960).
29. Emery, V. J. and A. M. Sessler, *Phys. Rev.* **119**, 43 (1960).
30. Anderson, P. W. and P. Morel, *Phys. Rev.* **123**, 1911 (1961).
31. Balian, R. and N. R. Werthamer, *Phys. Rev.* **131**, 1553 (1963).
32. Layzer, A. and D. Fay, *Int. J. Mag.* **1**, 135 (1971).
33. Grilly, E. R., E. F. Hammel and S. G. Sydoriak, *Phys. Rev.* **75**, 1103 (1949).
34. Lee, D. M. and H. A. Fairbank, *Phys. Rev.* **115**, 1359 (1959).
35. Lee, D. M., H. A. Fairbank and E. J. Walker, *Phys. Rev.* **121**, 1258 (1961).
36. Halperin, W. P., C. N. Archie, F. B. Rasmussen, R. A. Buhrman and R. C. Richardson, *Phys. Rev. Lett.* **32**, 927 (1974).
37. Pomeranchuk, I., *Zh. Eksp. i Teor. Fiz.* **20**, 919 (1950).
38. Straty, G. E., and E. D. Adams, *Rev. Sci. Instr.* **40**, 1393 (1969).
39. Tedrow, P. M. and D. M. Lee, *Phys. Lett.* **9**, 193 (1964).
40. Lipschultz, F. P. and D. M. Lee, *Phys. Rev. Lett.* **14**, 1017 (1965).
41. Grilly, E. R., S. G. Sydoriak and R. L. Mills, in *Helium Three*, ed. J. G. Daunt, Ohio State University Press, Columbus, Ohio (1960), p. 120.
42. Hall, H. E., P. J. Ford and K. Thompson, *Cryogenics* **6**, 80 (1966).
43. Wheatley, J. C., R. E. Rapp and R. T. Johnson, *J. Low Temp. Phys.* **4**, 1 (1971).
44. Sites, J. R., D. D. Osheroff, R. C. Richardson and D. M. Lee, *Phys. Rev. Lett.* **23**, 836 (1969).
45. Anufriyev, Yuri D., *Soviet Physics JETP Letters* **1**, 155 (1965).
46. Johnson, R. T., R. Rosenbaum, O. G. Symko and J. C. Wheatley, *Phys. Rev. Lett.* **22**, 449 (1969).
47. Wheatley, J. C., private communication.
48. Osheroff, D. D., R. C. Richardson and D. M. Lee, *Phys. Rev. Lett.* **28**, 885 (1972).
49. Lauterbur, P. C., *Nature* **242**, 190 (1973).
50. Osheroff, D. D., W. J. Gully, R. C. Richardson and D. M. Lee, *Phys. Rev. Lett.* **29**, 920 (1972).
51. Leggett, A. J., *Phys. Rev. Lett.* **29**, 1227 (1972).
52. Leggett, A. J., *Rev. Mod. Phys.* **47**, 331 (1975).
53. Leggett, A. J., *J. Phys. C* **6**, 3187 (1973).
54. Leggett, A. J., *Ann. Physics (New York)* **85**, 11 (1974).
55. Lee, D. M., *Proceedings of the 13th International Conference on Low Temperature Physics*, Boulder, Colorado, edited by K. D. Timmerhaus, W. J. O'Sullivan and E. F. Hammel (Plenum Press) 1972, Vol. 2, p. 25.
56. Osheroff, D. D., W. J. Gully, R. C. Richardson and D. M. Lee, *Proceedings of the 13th International Conference on Low Temperature Physics*, Boulder, Colorado, edited by K. D. Timmerhaus, W. J. O'Sullivan and E. F. Hammel (Plenum Press) 1972, Vol. 2, p. 134.
57. Alvesalo, T. A., Yu. D. Anufriyev, H. K. Collan, O. V. Lounasmaa and P. Wennerström, *Phys. Rev. Lett.* **30**, 962 (1973).
58. Yanof, A. and J. D. Reppy, *Phys. Rev. Lett.* **33**, 631 and 1030 erratum (1974).
59. Kojima, H., D. N. Paulson and J. C. Wheatley, *Phys. Rev. Lett.* **32**, 141 (1974).
60. Lawson, D. T., W. J. Gully, S. Goldstein, R. C. Richardson and D. M. Lee, *Phys. Rev. Lett.* **30**, 541 (1973).

61. Webb, R. A., T. J. Greytak, R. J. Johnson and J. C. Wheatley, *Phys. Rev. Lett.* **30**, 210 (1973).
62. Osheroff, D. D., Cornell University Ph.D thesis, (1973). See also Gully, W. J., D. D. Osheroff, D. J. Lawson, R. C. Richardson and D. M. Lee, *Phys. Rev. A* **8**, 1633 (1973).
63. Ambegaokar, V. and N. D. Mermin, *Phys. Rev. Lett.* **30**, 81 (1973).
64. Lawson, D. T., H. M. Bozler and D. M. Lee in *Quantum Statistics and the Many Body Problem*, ed. S. B. Trickey, W. P. Kirk and J. W. Duffy, Plenum Press, New York, 1975, p. 19.
65. Paulson, D. N., H. Kojima and J. C. Wheatley, *Phys. Rev. Lett.* **32**, 1098 (1974).
66. Ambegaokar, V., P. G. de Gennes and D. Rainer, *Phys. Rev. A* **9**, 2676 (1974); erratum, *ibid*, **A12**, 345 (1975).
67. Anderson, P. W. and W. F. Brinkman, *Phys. Rev. Lett.* **30**, 1108 (1973).
68. Rainer, D. and J. W. Serene, *Phys. Rev. B* **13**, 4745 (1976).
69. Lee, D. M. and R. C. Richardson in *The Physics of Liquid and Solid Helium*, ed. K. H. Bennemann and J. B. Ketterson, John Wiley and Sons, New York 1978, pp. 287-496.
70. Osheroff, D. D. and W. F. Brinkman, *Phys. Rev. Lett.* **32**, 584 (1974).
71. Bozler, H. M., M. E. R. Bernier, W. J. Gully, R. C. Richardson and D. M. Lee, *Phys. Rev. Lett.* **32**, 875 (1974).
72. Webb, R. A., R. L. Kleinberg and J. C. Wheatley, *Phys. Rev. Lett.* **33**, 145 (1974).
73. Mermin, N. D. and T. L. Ho, *Phys. Rev. Lett.* **36**, 594 (1976); erratum, *ibid*, **36**, 832 (1976).
74. Berthold, J. E., R. W. Giannetta, E. N. Smith and J. D. Reppy, *Phys. Rev. Lett.* **37**, 1138 (1976).
75. Lawson, D. T., H. M. Bozler and D. M. Lee, *Phys. Rev. Lett.* **34**, 121 (1975).
76. Roach, P. R., B. M. Abraham, P. D. Roach and J. B. Ketterson, *Phys. Rev. Lett.* **34**, 715 (1975).
77. Kurti, N., F. N. Robinson, F. Simon and D. A. Spohr, *Nature, London*, **178**, 450 (1956).
78. Dundon, J. M., D. L. Stolfi and John Goodkind, *Phys. Rev. Lett.* **30**, 843 (1973).
79. Ahonen, A. I., M. T. Haikala, M. Krusius and O. V. Lounasmaa, *Phys. Rev. Lett.* **33**, 628 (1974) and *ibid* **33**, 1595 (1974).
80. Wölffe, P., *Phys. Rev. Lett.* **30**, 1169 (1973) and *ibid* **31**, 1437 (1973).
81. Serene, J. W., Cornell University Ph.D thesis (1974).
82. Maki, K., *J. Low Temp. Phys.* **16**, 465 (1974).
83. Giannetta, R. W., A. Ahonen, E. Polturak, J. Saunders, E. K. Zeise, R. C. Richardson and D. M. Lee, *Phys. Rev. Lett.* **45**, 262 (1980).
84. Mast, D. B., B. K. Sarma, J. R. Owers-Bradley, I. D. Calder, J. B. Ketterson and W. P. Halperin, *Phys. Rev. Lett.* **45**, 266 (1980).
85. Avenel, O., E. Varoquaux and H. Ebisawa, *Phys. Rev. Lett.* **45**, 1952 (1980).
86. Movshovich, R., E. Varoquaux, N. Kim and D. M. Lee, *Phys. Rev. Lett.* **61**, 1732 (1988).
87. Tewordt, L. and N. Schopohl, *J. Low Temp. Phys.* **37**, 421 (1979), and N. Schopohl and L. Tewordt, *ibid* **45**, 67 (1981).
88. Avenel, O., M. E. Bernier, E. J. Varoquaux and C. Vibet in *Proceedings of the 14th International Conference on Low Temp. Physics*, ed. M. Krusius and M. Vuorio, North Holland, Amsterdam, 1975, p. 429.
89. Gould, C. M. and D. M. Lee, *Phys. Rev. Lett.* **37**, 1223 (1976).
90. Maki, K. and P. Kumar, *Phys. Rev. B* **16**, 182 (1977).
91. Corruccini, L. R. and D. D. Osheroff, *Phys. Rev. Lett.* **45**, 2029 (1980).
92. Gammel, P. L., H. E. Hall and John D. Reppy, *Phys. Rev. Lett.* **52**, 121 (1984).
93. Gammel, P. L., T. L. Ho and John D. Reppy, *Phys. Rev. Lett.* **55**, 2708 (1985).
94. Salomaa, M. M. and G. E. Volovik, *Reviews of Modern Phys.* **59**, 533 (1987).
95. Hakonen, P. J., M. Krusius, M. M. Salomaa, J. T. Simola, Yu. M. Bunkov, V. P. Mineev and G. E. Volovik, *Phys. Rev. Lett.* **51**, 1362 (1983), and Hakonen, P. J., M. Krusius and H. K. Seppälä, *J. Low Temp Phys.* **60**, 187 (1985).
96. Vinen, W. F., *Proc. Roy. Soc. A* **260**, 218 (1961).
97. Davis, J. C., J. D. Close, R. Zieve and R. E. Packard, *Phys. Rev. Lett.* **66**, 329 (1991).

98. Borovik-Romanov, A. S., Yu. Bunkov, V. V. Dmitriev, Yu. M. Mukharsky and D. A. Sergatskov, *Phys. Rev. Lett.* **62**, 1631 (1989), and Borovik-Romanov, A. S., Yu. M. Bunkov, A. de Vaard, V. V. Dmitriev, V. Makrotsieva, Yu. M. Mukharskii, and D. A. Sergatskov, *Soviet Phys. JETP Letters* **47**, 478, 1988.
99. Sigrist, M. and K. Ueda, *Reviews of Modern Phys.* **63**, 239 (1991).
100. Wollman, D. A., D. J. Van Harlingen, W. C. Lee, D. M. Ginsberg and A. J. Leggett, *Phys. Rev. Lett.* **71**, 2134 (1993).
101. Tsuci, C. C., J. R. Kirtley, C. C. Chi, L. S. Yu-Jahnes, A. Gupta, T. Shaw, T. Z. Sun and M. B. Ketchen, *Phys. Rev. Lett.* **73**, 593 (1994).
102. Lin, S.-W., C. Jin, H. Zhang, J. B. Ketterson, D. M. Lee, D. J. Hinks, M. Levy and B. K. Sarma, *Phys. Rev. B* **49**, 10001 (1994).
103. Oja, A. S. and O. V. Lounasmaa, *Rev. Mod. Phys.*, **69**, 1 (1997).
104. Sauls, J. A., D. Stein and J. W. Serene, *Phys. Rev. D* **25**, 967 (1982).
105. Volovik, G., *Exotic Properties of Superfluid ^3He* (World Scientific, Singapore 1992).
106. Ruutu, V. M. H., V. B. Eltsov, A. J. Gill, T. W. B. Kibble, M. Krusius, Yu. G. Makhlin, B. Placais, G. E. Volovik and W. Xu, *Nature* **382**, 334 (1996).
107. Bäuerle, G., Yu. M. Bunkov, S. N. Fisher, H. Godfrin and G. R. Pickett, *Nature* **382**, 332 (1996).
108. Bevan, T. D. C., A. J. Manninen, J. B. Cook, J. R. Hook, H. E. Hall, T. Vachaspati and G. E. Volovik, preprint, submitted to *Nature*.